KfK 3917
Mai 1985

Reaction Kinetics of Zircaloy-4 in a 25% O_2/75% Ar Gas Mixture from 900 to 1500° C under Isothermal Conditions

H. Uetsuka, P. Hofmann
Institut für Material- und Festkörperforschung
Projekt Nukleare Sicherheit

Kernforschungszentrum Karlsruhe

KERNFORSCHUNGSZENTRUM KARLSRUHE
Institut für Material- und Festkörperforschung
Projekt Nukleare Sicherheit

KfK 3917

Reaction Kinetics of Zircaloy-4 in a 25% O_2/75% Ar Gas Mixture from 900 to 1500°C under Isothermal Conditions

H. Uetsuka*, P. Hofmann

in cooperation with

J. Burbach
H. Metzger

Kernforschungszentrum Karlsruhe GmbH., Karlsruhe

* Japan Atomic Energy Research Institute, Tokai-mura, Ibaraki-ken, 319-11, presently delegated to the Kernforschungszentrum Karlsruhe

Kernforschungszentrum Karlsruhe GmbH
ISSN 0303-4003

Summary

The reaction kinetics of Zircaloy-4 in oxygen and argon were determined by isothermal oxidation tests of cladding specimens at temperatures from 900 to 1500°C for times between 2 and 60 minutes. In this temperature range the oxidation reaction obeys a parabolic rate law. A discontinuity in the temperature dependence of the reaction rate was observed between 1000 and 1100°C, which may be attributed to an allotropic phase transformation of the ZrO_2. The equations describing the temperature dependence of the parabolic rate constants for mass increase, ZrO_2 oxide layer growth and (ZrO_2 + α-Zr(O)) double layer growth were determined.

No significant difference was seen between the oxidation rate equations obtained in the present study and those obtained in the Zircaloy-4/steam oxidation experiments. Changing the oxygen concentration in the gas mixture from 10 to 100 vol% does not affect the oxidation kinetics of Zircaloy-4.

Finally, an evaluation was made of the temperature measured in the MONA experiments (UO_2/Zircaloy-4 interaction experiments under oxidizing conditions) using the reaction kinetics for oxide layer growth obtained in the present experiments. The comparison of the ZrO_2 oxide layer thickness for certain time-temperature curves shows that the temperatures in the MONA tests determind, using a pyrometer, were 25 to 70°C below the actual test temperature in the temperature range from 1000 to 1400°C.

Reaktionskinetik zwischen Zircaloy-4 und einem 25% O_2/75% Ar Gasgemisch im Temperaturbereich von 900 bis 1500°C

Zusammenfassung

Im Temperaturbereich von 900 bis 1500°C wurde die Reaktionskinetik zwischen Zircaloy-4 und einem Sauerstoff-/Argon-Gasgemisch in isothermen Versuchen bestimmt. Die Reaktionszeit variierte zwischen 2 und 60 Minuten. In dem untersuchten Temperaturbereich erfolgt die Oxidation nach einem parabolischen Zeitgesetz. Die Temperaturabhängigkeit der Reaktionsgeschwindigkeit zeigt eine Unstetigkeit zwischen 1000 und 1100°C, die sehr wahrscheinlich durch eine allotrope Phasenumwandlung des ZrO_2 verursacht wird. Es wurden die temperaturabhängigen Reaktionsgleichungen für die Gewichtszunahme sowie für das Wachstum der ZrO_2-Oxidschicht und der (ZrO_2+ α-Zr(O))-Doppelschicht bestimmt.

Zwischen den in dieser Arbeit bestimmten Reaktionsgleichungen und denen von Zircaloy/Wasserdampf Oxidationsexperimenten bestehen keine wesentlichen Unterschiede. Die Oxidationskinetik von Zircaloy hängt nicht vom Sauerstoffgehalt der untersuchten Gasmischungen (10 bis 100 Vol.%) ab.

Ziel der Experimente war es, u.a. die in den MONA-Experimenten (UO_2/Zircaloy-4-Reaktionsexperimente unter oxidierenden Versuchsbedingungen) mit einem Pyrometer gemessenen Temperaturen zu überprüfen. Es wurden daher die Oxidschichtdicken der MONA-Experimente mit denen in dieser Arbeit ermittelten Werten für bestimmte Temperatur-Zeit-Kombinationen verglichen. Dabei zeigte sich, daß die in den MONA-Versuchen gemessenen Temperaturen im Temperaturbereich von 1000 bis 1400°C ca 25 bis 70°C unterhalb der tatsächlichen Probentemperaturen lagen.

Content

Tables

Figures

Fig. 1: Gas flow rate as a function of the scale of flow meter. (25 Vol.% Oxygen + 75 Vol.% Argon, Rotameter Nr. L 6.3/250-4221).

Fig. 2: Axial temperature profile in the test furnace.

Fig. 3: Temperature transient for isothermal oxidation test at 1400°C for 2 min and normalization to equivalent isothermal oxidation time.

Fig. 4: Visual appearance of Zircaloy-4 specimens oxidized at 996 and 1100°C for 2 to 60 min.

Fig. 5: Oxide (ZrO_2) film formed uniformly along the specimen length. Oxidation at 1400°C for 15 min.

Fig. 6: Photomicrographs of Zircaloy-4 oxidized at 1300°C for 2 to 15 min in a (25 Vol.% O_2/75 Vol.% Ar) gas mixture.

Fig. 7: Photomicrographs of Zircaloy-4 oxidized at 1300°C for 20 to 60 min in a (25 Vol.% O_2/75 Vol.% Ar) gas mixture.

Fig. 8: Photomicrographs of Zircaloy-4 oxidized at 1500°C for 2 to 10 min in a (25 Vol.% O_2/75 Vol.% Ar) gas mixture.

Fig. 9: Photomicrographs of Zircaloy-4 oxidized at 1500°C for 15 to 30 min in a (25 Vol.% O_2/75 Vol.% Ar) gas mixture.

Fig. 10: Mass increase of Zircaloy-4 cladding specimens oxidized at different temperatures versus the square root of oxidation time ($\sqrt{t}$).

Fig. 11: Increase of oxide (ZrO_2) layer thickness as a function of the square root of oxidation time ($\sqrt{t}$).

Fig. 12: Increase of (ZrO_2+α-Zr(O)) double layer thickness as a function of the square root of oxidation time ($\sqrt{t}$).

Fig. 13: Arrhenius plot of the parabolic rate constants for mass increase from 900 to 1500°C.

Fig. 14: Arrhenius plot of the parabolic rate constants for oxide layer growth from 900 to 1500°C.

Fig. 15: Variation of layer thickness ratio of ZrO_2/oxygen-stabilized α-Zr(O) as a function of oxidation time.

Fig. 16: Arrhenius plot of the parabolic rate constants for (ZrO_2+ α-Zr(O)) layer growth from 900 to 1400°C.

Fig. 17: Comparison of oxidation rate of Zircaloy-4 measured in steam and in a (25 Vol.% O_2/75 Vol.% Ar) gas mixture (present work).

Fig. 18: Mass increase of Zircaloy-4 cladding specimens oxidized at 1200°C as a function of the square root of oxidation time ($\sqrt{t}$) at three different oxygen to argon ratios.

Fig. 19: Correlation between nominal test temperatures in the MONA experiments and the temperatures evaluated from the oxide layer thickness.

1. Introduction

Evaluating severe accidents of light water reactors, requires detailed knowledge of the chemical interactions and reaction kinetics between UO_2 fuel and Zircaloy-4 (Zry) cladding as well as between steam and Zry at high temperatures. Extensive out-of-pile UO_2/Zry interaction experiments have been performed at temperatures ranging from 900 to 1700°C in the high temperature/high pressure MONA facility under inert conditions (Ar) /1,2/ and oxidizing conditions (Ar + O_2) /14,15/. The results obtained to date have been used in developing computer codes describing the chemical interactions.

In the MONA experiments /1,2,14,15/ non-contact temperature measurements were performed using an infrared and an emissivity-insensitive dual wavelength pyrometer. In general, it is difficult to make accurate temperature measurements in tests performed at high temperatures. Therefore, when possible, the measured temperature should be checked by another method. In the case of the isothermal oxidation of Zry, it is possible to determine the cladding temperature from the time at temperature and the thickness of the oxide (ZrO_2) layer which forms on the surface of the specimen. However, accurate kinetics data for the oxide layer growth due to the Zry/oxygen reaction are needed.

The Zry/steam reaction has already been widely investigated for the large break loss-of-coolant accident (LOCA) analysis, and reliable kinetics data are available /3/through /6/. However, the Zry/steam kinetics data may not be directly applicable for the temperature evaluation of the MONA experiments, since these tests were run in a 25 Vol.% O_2/75 Vol.% Ar gas mixture. The oxidation kinetics of Zry in the gas mixture must first be determined accurately and precisely and then these data can be used for the determination of the temperatures in the MONA experiments.

This report describes the results of Zircaloy-4 oxidation experiments conducted at temperatures ranging from 900 to 1500°C in a 25 Vol.% oxygen/75 Vol.% argon gas mixture. Tests were also performed with

different argon to oxygen ratios to check if the gas composition has an influence on the reaction kinetics. In addition, some examples are given in which the kinetics data are used to evaluate MONA test temperatures /14,15/.

2. Experiment Design and Conduct

2.1. Specimen and Apparatus

The chemical composition of the Zry-4 used in the oxidation experiments is listed in Table 1. Tubular specimens 10 mm in length were cut from PWR size Zry-4 cladding with a 10.75 mm O.D. and 9.30 mm I.D. Prior to testing, the specimens were degreased in acetone. The test apparatus consisted of a 25 mm I.D. alumina reaction tube, an electric resistance tube furnace and a gas supply system.

2.2. Experimental Procedure

Before each oxidation test, the apparatus was purged with an oxygen-argon gas-mixture. The furnace and reaction tube were first stabilized at the desired test temperature. The specimen was then inserted into the midpoint of the tubing and oxidized in a flowing gas mixture of 25 Vol.% oxygen and 75 Vol.% argon.

The flow rate of the gas mixture was measured with a flow meter (Fig. 1) and a constant rate ranging from 30 to 70 ml/s was maintained during each test. The flow rate was set at least a factor of two above the actual rate required. This was calculated using the following empirical expression /7/ (1) for the oxygen uptake of Zry-4 in an unlimited steam flow,

$$\tau = 0.724 \sqrt{t} \exp(-10481/T) \qquad (1)$$

where τ : oxygen uptake (g/cm^2)
t : oxidation time (s)
T : oxidation temperature (K).

The axial temperature difference in the center 40 mm of the furnace remained within ± 1°C during the test and was considered to be sufficiently uniform for oxidation experiment of small-sized tube specimen. The axial temperature distribution in the reaction tube of the furnace is shown in Figure 2. In each test the temperature of the tube specimen was measured with a Pt-10% Rh/Pt thermocouple attached to the inner cladding surface at its mid-point. The specimens were isothermally oxidized at temperatures ranging from 900 to 1500°C in steps of 100°C. Temperature overshooting of the specimens during heatup due to the exothermic reaction between Zry and oxygen was successfully avoided, when necessary, by shifting the specimens axially within the reaction tube. After the predetermined annealing time (between 2 and 60 minutes) the specimens were quickly pulled out of the hot zone and cooled-down.

2.3. Evaluation

The weight of each specimen was measured with a direct reading balance before and after annealing and the mass increase per unit area due to oxidation was calculated. All the oxidized specimens were examined metallographically to determine the thickness of the ZrO_2 oxide layer and the oxygen-stabilized α-Zr(O) layer.

In performing these oxidation tests the heat-up, cool-down, and thermal stabilization of the specimen are included in the overall oxidation. Therefore, the isothermal annealing time requires an appropriate correction. This correction normalizes the integral temperature-time excursion to an equivalent isothermal time at the predetermined oxidation temperature. In the present work, a simple method of temperature-time normalization of the experiments was used to estimate the isothermal oxidation time of each test. It is described below and shown in Figure 3. The mechanism which governs the oxidation of Zry is the diffusion of oxygen anions through the anion-deficient ZrO_2 lattice. The reaction rate at high temperatures is described by a parabolic expression of the form

$$w^2 = K_p \cdot t \qquad (2)$$

where w = measure of the extent of the reaction

t = reaction time

K_p = parabolic reaction rate constant.

The parabolic rate constant, K_p, is related to temperature by an Arrhenius equation,

$$K_p = A \exp(-Q/RT) \qquad (3)$$

where A is the pre-exponential term, Q is the activation energy, R is the universal gas constant and T is the absolute temperature. Leistikow and Schanz /7,8/ reported that the oxidation kinetics of Zry-4 in steam can be described by this expression (3) over the temperature range 600 to 1500°C and for oxidation times of up to 15 minutes. If one assumes that the rate constants for the oxidation kinetics of Zry-4 in these tests follow an Arrhenius relationship, the equivalent isothermal annealing time at an assigned temperature is calculated by the following equation /3/:

$$t_{eq} = \frac{\int_0^t \exp[-Q/RT(t)]\, dt}{\exp(-Q/RT_{as})} \qquad (4)$$

where t_{eq} = equivalent time, s, at an assigned temperature, T_{as}

T_{as} = assigned temperature, K

$T(t)$ = actual temperature, K, as a function of time

Q = activation energy

R = universal gas constant, 8.314 J/mol·K

t = time, s.

The integral form for the equivalent annealing time can be approximately represented by the following series,

$$t_{eq} = t_s \frac{\sum_{i=1}^{n} \exp\ (-Q/RT_i)}{\exp\ (-Q/RT_{as})} \qquad (5)$$

where t_s = time step, s

T_i = average temperature at each time step, K.

For these tests a time step t_s of 2s was used and the correction of the temperature transient below 600°C was generally neglected, since only negligible oxidation occurs, and the activation energy of 174.3 kJ/mol obtained by Leistikow et.al /7/ was applied. Additional calculations were performed for some selected cases with a 5s time step in order to check the change in the calculated results (t_{eq}) due to the different time step. No significant changes in the results were obtained by using the larger time step.

An example of a temperature transient and its normalization is shown in Fig. 3. The test temperature in this case was 1400°C and the desired equivalent time at 1400°C was 2 minutes. As is seen in Figure 3, the actual time at 1400°C was about 90 seconds. However, the equivalent isothermal oxidation time at 1400°C is estimated to be 137 seconds. Similar equivalent isothermal oxidation times were determined in this way for each test and these are used in the kinetics data calculations.

3. Experimental Results

The visual appearance of Zircaloy-4 specimens oxidized at 996 and 1100°C for durations ranging from 2 to 60 minutes are shown in Figure 4. A black oxide film is seen on the surface of all of the specimens oxidized at 1100°C. At 996°C, however, gray oxide films are seen to form locally on the surfaces of the specimens oxidized for more than 30 minutes. This can be interpreted as the result of an early breakaway transition at this temperature as was reported by Schanz et.al /9/.

To check the uniformity of the oxide layer thickness along the specimen length, selected specimens were cut axially and examined metallographically. Figure 5 shows the optical photomicrographs of a typical specimen oxidized at 1400°C for 15 minutes. The sample here is in the as-polished condition. No significant axial dependence of the oxide layer thickness was seen in any of the specimens. This confirms the assumption that enough oxygen is available for uniform axial and circumferential oxidation of the specimens under the applied gas flow conditions.

The principal objective of these experiments is to evaluate the oxidation kinetics, that means the time-temperature dependence of the oxide layer growth rate. It was therefore necessary to determine the oxide layer thickness as a function of temperature and time. The thickness of both the ZrO_2 oxide layer and the (ZrO_2+α-Zr(O)) double layer were measured directly on metallographically prepared specimens with an optical microscope, and a minimum of six different orientations were measured. Optical photomicrographs of specimens oxidized at 1300 and 1500°C are shown in Figures 6 through 9 in the as-polished condition. At temperatures above the allotropic α/β phase transformation of zirconium [above the (α+β)/β transformation temperature of Zr alloys], the oxygen reacts with β-Zr to form a ZrO_2 surface layer and an intermediate layer of oxygen-stabilized α-Zr(O). The boundary between the α-Zr(O) and the remainder of the cladding (prior β-Zry) is generally distinct. However it can be very irregular in places where α-Zr(O) incursions extend into the prior β-Zr, especially at higher oxidation temperatures and longer annealing times. In the tests at 1300°C the thickness of the α-Zr(O) layer could be measured on only the two specimens oxidized for 2 and 5 minutes (Fig. 6). The Zry/oxygen reaction rates increase rapidly with increasing temperature. For example, the Zry-4 cladding specimen (0.73 mm wall thickness) was completely oxidized to ZrO_2 within 30 minutes at 1500°C (Fig. 9). The kinetics data obtained in these tests are, therefore, not necessary valid for long oxidation times at high temperatures.

The mass increase, ZrO_2 oxide layer thickness and (ZrO_2+α-Zr(O)) double layer thickness measured in each experiment are listed in Table 2 together with the experimental conditions. The thickness of oxide layer

and (ZrO_2+α-Zr(O)) double layer listed in the table are average values calculated for each specimen.

The mass increase of the Zry-4 cladding specimens oxidized at different temperatures as a function of the square root of the isothermal oxidation time is shown in Figure 10. A linear relationship was found between the mass increase and the square root of oxidation time at every test temperature. Therefore, the reaction rate follows parabolic kinetics confirming that the chemical interaction between Zry-4 and oxygen is a diffusion-controlled process. The parabolic rate constants, which correspond to the slopes of the lines, are determined at each temperature graphically or by a linear regression method using the method of the least squares (Tables 3 through 5).

The correlation between the thickness of the oxide layer and the square root of oxidation time is shown in Figure 11. Also in this case, a linear relationship is found. The large scattering in the data at 996°C and at long oxidation times (45 and 60 minutes) can be interpreted as a result of an early breakaway transition /9/ which is typical at this temperature (see Figure 4). At high temperatures and long oxidation times, the experimental data deviates from a linear relationship. For example, at 1300°C the data at 45 and 60 minutes deviate from the linear regression line (Figure 11). This deviation is presumably due to the finite wall thickness of the cladding specimen. However, the parabolic rate constants for oxide layer growth can be determined without significant errors at these temperatures for a limited oxidation time, e.g. between 2 and 30 minutes at 1300°C.

Figure 12 shows the correlation between the double layer thickness of ZrO_2 and oxygen-stabilized α-Zr(O) and the square root of isothermal oxidation time. The linear relationship between the thickness of the (ZrO_2+α-Zr(O)) double layer and the square root of time is clearly seen. The large scatter of the data at 996°C at the oxidation times of 45 and 60 minutes can again be interpreted as a

result of an early breakaway transition /9/. The boundary between the oxygen-stabilized α-Zr(O) layer and the prior β-Zr was not distinct for most of the specimens oxidized at the temperatures above 1300°C and longer annealing times. The thickness of (ZrO_2+α-Zr(O)) double layer could be measured on only three of the specimens oxidized at 1300 and 1400°C. Therefore, the parabolic rate constants for the (ZrO_2+α-Zr(O)) double layer growth at these temperatures are valid only for short oxidation times, e.g. up to 5 minutes at 1300°C.

4. Discussion

4.1. Reaction Kinetics

It is generally accepted that the rate determining step of the Zry-oxygen reaction is the diffusion of oxygen anions in the oxygen deficient ZrO_2 lattice. The linear relationship between the measured values such as mass increase and the square root of the oxidation time (figs. 10,11 and 12) shows that the Zry/oxygen reaction obeys a parabolic rate law indicating a diffusion controlled reaction.

The Tables 3 and 4 list the parabolic rate constants obtained for the mass increase, the ZrO_2 oxide layer growth and the (ZrO_2+α-Zr(O)) double layer growth over the temperature range 900 to 1500°C.

As mentioned in section 3, these rate constants are valid only for limited oxidation times. The range of annealing times for each isotherm is also included in Tables 3 and 4. The equations describing the temperature dependence of the parabolic rate constants are listed in Table 5.

The temperature dependence of the parabolic rate constant for the mass increase, K_w, is shown in an Arrhenius plot in Figure 13. It is possible to draw one straight line through all the data points in the examined temperature range. However, a better fit is obtained when the data points are divided into two sections as shown in Fig. 13. The discontinuity in the temperature dependence may be attributed to an allotropic phase transformation of the ZrO_2. The Zr-O phase diagram /10/indi-

cates that β-Zr reacts with oxygen at high temperatures to form a layer of oxygen-stabilized α-Zr(O), a layer of cubic ZrO_2 and a layer of tetragonal ZrO_2 above the eutectoid transformation temperature at about 1580°C. When cooled through this transformation temperature the cubic ZrO_2 undergoes a eutectoid decomposition to tetragonal ZrO_2 and metallic α-Zr(O) which forms within the ZrO_2. On further cooling the tetragonal ZrO_2 undergoes another eutectoid decomposition into stable monoclinic ZrO_2 and α-Zr(O) at about 1000°C. Urbanic and Heidrick /11/ reported that there was a discontinuity in the temperature dependence of the reaction rate of Zry-4 and steam at about 1580°C and they attributed this to the change in the oxide phase. Aly /12/ showed a similar discontinuity in the temperature dependence of the parabolic rate constants of the Zry/steam reaction at a temperature of about 1550°C. Such discontinuities are reasonable, since the mechanism which governs the oxidation of Zry is the diffusion of oxygen anions through the ZrO_2 lattice and the diffusion coefficient of oxygen should change when the crystal structure of the ZrO_2 changes. Consequently, a discontinuity in the temperature dependence of the parabolic rate constants is also possible at the temperature of the tetragonal to monoclinic phase transformation. The Zry/steam reaction has been extensively investigated and a broad range of kinetics data /3 through 6/ are available. However, a discontinuity due to the phase transofrmation of tetragonal ZrO_2 into monoclinic ZrO_2 at lower temperatures has not been reported before.

In the work of Cathcart et. al /3/, a slight deviation of the data from the Arrhenius plot (logaritms of the parabolic rate constants versus reciprocal temperature) can be seen at 1000°C. The equations obtained in this study describing the temperature dependence of the parabolic rate constants for the mass increase are given as follows (Table 5):

$$K_W = 24.12 \exp(-211{,}112/RT) \quad \text{for} \quad 900 - 1100^{\circ}C,$$

and

$$K_W = 0.135 \exp(-152{,}805/RT) \quad \text{for} \quad 1100 - 1500^{\circ}C.$$

The units of the parabolic rate constants, K_w, are $g^2/cm^4 \cdot s$, the universal gas constant R = 8.314 J/mol.K and T is the absolute temperature in K.

Figure 14 is an Arrhenius plot of the parabolic rate constant, K_δ, (ZrO_2 layer thickness) versus reciprocal temperautre, 1/T; the determined temperature dependent correlations are listed in Table 5. A good linear relationship between the logarithms of the parabolic rate constants and the reciprocal temperature is seen in the temperature range of 900 to 1100°C. However, the rate constants deviate from a linear plot above 1100°C, and the deviation of the data points from the regression line (dotted line in Fig. 14) is obvious at 1400 and 1500°C. This non linearity at high temperatures is possibly due to the following. The Zry/oxygen reaction rate is so fast at high temperatures that the β-phase layer of the cladding specimen will disappear in a few minutes (see Fig. 8). Therefore, the increase rate of oxygen concentration in the α-Zr(O) layer is higher at longer oxidation times than that at the initial oxidation stage of a few minutes (double-sided oxidation of the tube specimens). This could result in a rapid growth of the oxide layer. Biederman et. al /13/ reported that at high temperatures (in excess of 1480°C) rapid oxide growth occurs which trapps oxygen-stabilized α-Zr(O) in the ZrO_2 layer. The irregular phase boundary between the ZrO_2 and the α-Zr(O) layer shown in Fig. 8 (photomicrographs of specimens oxidized at 1500°C) suggests such trapping of α-Zr(O) in the ZrO_2 during oxidation. The temperature dependence of the rate constants for oxide layer growth can be divided into three sections in the temperature range shown in Fig. 14. However, the deviation of the data from the regression lines is not negligible at temperatures from 1100 to 1500°C. Therefore, the following five equations for the parabolic rate constant K_δ (thickness of the ZrO_2 layer) were determined by a point-by-point analysis (Table 5) for the temperature evaluations of the MONA experiments (4.4).

$K_\delta = 21.52 \exp(-222{,}682/RT)$ for 900 - 1100°C

$K_\delta = 8.27 \cdot 10^{-4} \exp(-107{,}230/RT)$ for 1100 - 1200°C

$K_\delta = 6.14 \cdot 10^{-3} \exp(-131{,}775/RT)$ for 1200 - 1300°C

$K_\delta = 0.259 \exp(-180{,}709/RT)$ for 1300 - 1400°C

$K_\delta = 158.2 \exp(-269{,}890/RT)$ for 1400 - 1500°C

The variation in the ratio of the ZrO_2 layer thickness versus the oxygen-stabilized α-Zr(O) layer thickness is shown in Figure 15 as functions of oxidation time and temperature. At 900°C, the ratio falls between 1.1 to 1.2 for oxidation times up to 20 minutes and then decreases with increasing time to between 0.9 to 1.0. The ratio at 996°C varies between 1.6 to 1.7, which is the highest value obtained in these tests. At higher temperatures, the ratio decreases with increasing temperature and falls between 0.7 to 0.8 at 1300 and 1400°C. The relative ratio of ZrO_2 oxide layer thickness to the thickness of oxygen-stabilized α-Zr(O) layer varies considerably depending on the oxidation temperature.

The temperature dependence of the parabolic rate constants for the (ZrO_2+α-Zr(O)) double layer growth (K_ξ) is shown in an Arrhenius plot in Figure 16. The rate constant has a linear dependence on the reciprocal temperature 1/T in the temperature ranges above and below 1100°C. The equations describing the temperature dependence of K_ξ are calculated for both temperature ranges as follows:

$K_\xi = 14.96 \exp(-207{,}521/RT)$ for 900 - 1100°C,

$K_\xi = 1.549 \exp(-181{,}885/RT)$ for 1100 - 1400°C.

where K_ξ is in cm^2/s, R = 8.341 J/mol·K, and T in K.

4.2. Comparison of Zry/Oxygen Kinetics with Zry/Steam Kinetics

A general comparison of the results obtained in this investigation with the results obtained in the Zry/steam oxidation experiments is made in terms of the parabolic rate constants obtained for mass in-

crease (K_w). The rate constants K_w reported by several investigators are given below.

Present investigation:

$$K_w = 24.12 \exp(-211,112/RT) \text{ for } 900 - 1100^{\circ}C$$

$$K_w = 0.135 \exp(-152,805/RT) \text{ for } 1100 - 1500^{\circ}C$$

Cathcart et al./3/:

$$K_w = 0.362 \exp(-167,117/RT) \text{ for } 1000 - 1500^{\circ}C$$

Kawasaki et al./4/:

$$K_w = 0.468 \exp(-170,339/RT) \text{ for } 1000 - 1330^{\circ}C$$

Leistikow et al./5/:

$$K_w = 0.524 \exp(-174,284/RT) \text{ for } 900 - 1300^{\circ}C$$

Ballinger et al./6/:

$$K_w = 0.038 \exp(-139,627/RT) \text{ for } 982 - 1482^{\circ}C$$

The units of the parabolic rate constants, K_w, are given in $g^2/cm^4 \cdot s$, the universal gas constant R = 8·314 J/mol·K and T is the absolute temperature. While significant variations exist in both the pre-exponential and exponential terms of the various Arrhenius expressions, the rate constants calculated by these equations lie within a comparatively narrow data band over the temperature range where they apply. These rate constants are shown in Figure 17. The kinetics data obtained by Cathcart et al./3/ are considered to be the most reliable ones for the Zry/steam reaction and for this reason they are used in some computer codes for accident analysis. The data of Kawasaki et al./4/ agree very well with Cathcart's data /3/. The present oxidation kinetics data are slightly higher than the Zry/steam data at 1100 and 1200°C. However, they are in very good agreement with the data of Cathcart above 1300°C and also at 1000°C. At 900°C, Zry/oxygen kinetics data agree very well with the kinetics

data of Leistikow /5/. From this, the conclusion is drawn that there is no significant difference between the Zry oxidation kinetics in steam and Zry oxidation kinetics in a 25 Vol.% O_2/75 Vol.% Ar mixture from 900 to 1500°C. In the MONA experiments under oxidizing conditions /14,15/, the outer surface of Zry cladding specimen was exposed to a 25 Vol.% O_2/75 Vol.% Ar gas mixture, which is used to simulate a steam environment. In terms of the oxidation kinetics, this gas mixture has been found to be appropriate.

4.3. Influence of Oxygen Concentration in Gas Mixture on Reaction Kinetics

In the MONA experiments under oxidizing conditions /14,15/, described in section 4.2, the outer surface of the cladding specimen is exposed to a 25 Vol.% O_2/75 Vol.% Ar gas mixture. This gas mixture is continuously supplied into the high pressure reaction chamber during the test. However, the oxygen concentration of the gas mixture inside the apparatus is expected to decrease somewhat, especially in cases of Zry oxidation at very high temperatures, when the oxygen is consumed rapidly. Therefore, it is important to investigate the influence of the oxygen concentration in the gas mixture on the kinetics of Zircaloy/oxygen reaction.

The high temperature oxidation behavior of metals is dominated by the property of oxide film formed on the metal surface. The oxidation is controlled by mass transfer through the oxide film when a dense and uniform film is formed on the metal surface and the interactions at the metal/oxide/gas interfaces proceed at a sufficiently high rate. The growth rate of oxide film depends on both the gradient of defect concentration in the film and the diffusion rate. It is generally known that the oxidation rates of metals which forms n-type (anion-deficient) oxide do not depend on the oxygen partial pressure. ZrO_2 is classified as a n-type oxide. Consequently, if enough oxygen is supplied at the interface between the oxide and gas phase during oxidation the difference in oxygen concentration in the atmosphere will not affect the oxidation rate of Zry-4. However, this must be proved experimentally. To do this, oxidation tests of Zry-4 specimens were performed at 1200°C in two gas mixtures of 10 Vol% O_2/ 90

Vol.% Ar and 25 Vol.% O_2/75 Vol.% Ar, and in pure oxygen. The results of these tests are listed in Table 6 and the mass increase is plotted versus the square root of oxidation time in Figure 18 for three different gas mixtures. No significant difference was found for the mass increase of the specimens in the various gas mixtures, and the linear relationship between mass increase and $\sqrt{t}$ is valied for all these tests. Therefore, it is concluded that, when enough oxygen is supplied at the interface of the oxide and the gas phase ($\geq$ 10 Vol.% O_2), the oxygen concentration in the (oxygen + argon) gas mixture does not affect the Zry-4 oxidation kinetics.

4.4. Evaluation of Test Temperatures in the MONA Experiments

In the MONA experiments under oxidizing conditions /14,15/, the Zircaloy-4 cladding specimens are tested in a mixture of 25 Vol.% O_2/ 75 Vol.% Ar and the test temperature is measured with an infrared pyrometer. Accurate high temperature measurements are difficult and when possible the measured temperatures should be checked by an independent method. In the case of the isothermal oxidation of Zry, it is possible to determine the specimen temperature for a given time at temperature from the thickness of the oxide layer which forms on the specimen surface. The kinetics for oxide layer growth in a mixture of 25 Vol.% O_2/75 Vol.% Ar is accurately determined for the temperature range from 900 to 1500°C in section 4.1 and the nominal test temperature of the MONA experiments /14,15/ can be estimated using these kinetics data. The thickness of the oxide film is described by a parabolic expression of the form

$$\delta^2 = K_\delta t \qquad (6)$$

where

δ = thickness of oxide film
t = oxidation time
K_δ = parabolic rate constant for oxide film growth.

And the equation describing the temperature dependence of the parabolic rate constants is as follows,

$$K_\delta = A \exp(-B/RT) \qquad (7)$$

where R is the universal gas constant and T is the absolute temperature. Both the pre-exponential and exponential terms of the equation are given in section 4.1 for each temperature range. By using these two equations and the time at temperature, the isothermal oxidation temperature can be obtained from the thickness of the oxide film.

The estimated temperatures are listed in Table 7 together with the experimental data of MONA. Figure 19 shows the correlation between the measured test temperatures of the MONA experiments and the temperatures obtained from the oxide film thickness. No difference is observed between the pyrometrically measured and the estimated temperature at 900°C. However, obvious differeneces are seen above 1000°C. The temperature difference at 1200°C is between 50 to 70°C and the difference at 1400°C is found to be about 25°C. Therefore, this evaluation shows that the actual test temperature was higher than the indicated test temperature in most of the MONA experiments /14,15/ and need to be corrected.

5. Conclusions

Oxidation tests of Zircaloy-4 were performed at temperatures from 900 to 1500°C for times between 2 and 60 minutes in a gas mixture of 25 Vol.% oxygen and 75 Vol.% argon to determine the reaction kinetics of Zircaloy-4. The kinetics data were used to evaluate the pyrometrically measured test temperatures in the MONA experiments. The following conclusions are drawn from the test results:

(1) In the examined temperature range, the reaction obeyed a parabolic rate law.

(2) A discontinuity in the temperature dependence of the parabolic rate constants was observed between 1000 and 1100°C, which can be attributed to an allotropic phase transformation of the ZrO_2.

(3) The equations describing the temperature dependence of the parabolic rate constants for mass increase (oxygen uptake) are as follows:

$K_W = 24.12 \exp(-211{,}112/RT)$ for 900 - 1100°C,

$K_W = 0.135 \exp(-152{,}805/RT)$ for 1100 - 1500°C,

The units of the parabolic rate constants, K_W, are given in $g^2/cm^4 \cdot s$, the universal gas constant R = 8.314 J/mol·K and T is the absolute temperature.

(4) Comparisons of the oxidation rates obtained in the present study with those obtained in the Zircaloy/steam oxidation experiments show no significant difference.

(5) Changing the oxygen concentration between 10 and 100 Vol.% in the gas mixture does not affect the oxidation kinetics of Zircaloy-4.

(6) It was demonstrated by the temperature evaluation that the test temperatures in the MONA experiments (UO_2/Zry interaction experiments under oxidizing conditions /14,15/) were underestimated by about 25 to 70°C in the temperature range between 1000 and 1400°C.

6. Acknowledgment

We wish to thank Dr. B.J. Buescher (EG+G, Idaho) for his thorough review of the manuscript and his critical suggestions.

7. References

/1/ P. Hofmann, D. K. Kerwin-Peck, UO_2/Zircaloy-4 Chemical Interactions and Reaction Kinetics from 1000 to 1700°C under Isothermal Conditions (Final Report), KfK 3552, November 1983.

/2/ P. Hofmann and D.K. Kerwin-Peck, UO_2/Zircaloy-4 Chemical Interactions from 1000 to 1700°C under Isothermal and Transient Temperature Conditions, Journal of Nuclear Materials, 124, 1984, pp. 80-105.

/3/ J.V. Cathcart, R.E. Pawel, R.A. McKee, R.E. Druschel, G.J. Yurek, J.J. Campbell, S.H. Jury, Zirconium Metal-Water Oxidation Kinetics IV. Reaction Rate Studies, ORNL/NUREG-17, August, 1977.

/4/ S. Kawasaki, T. Furuta, M. Suzuki, "Oxidation of Zircaloy-4 under High Temperature Steam Atmosphere and Its Effect on Ductility of Cladding", Journal of Nuclear Science and Technology, 15(8), 1978, pp. 589-596.

/5/ S. Leistikow, G. Schanz, H.v. Berg, Kinetik und Morphologie der isothermen Dampf-Oxidation von Zircaloy-4 bei 700 - 1300°C, KfK 2587, March 1978.

/6/ R.G. Ballinger, W.G. Dobson, R.R. Biederman, "Oxidation Reaction Kinetics of Zircaloy-4 in an Unlimited Steam Environment", Journal of Nuclear Materials, 62, 1976, pp. 213-220.

/7/ S. Leistikow, G. Schanz, "High Temperature Oxidation of Zircaloy-4 Cladding Tubes in Steam (600-1600°C)", 9th International Congress on Metallic Corrosion, Toronto, Canada, June 3-7, 1984.

/8/ G. Schanz, private communication.

/9/ G. Schanz, S. Leistikow, "ZrO_2-Scale Degradation during Zircaloy-4 High Temperature Steam Exposure. Microstructural Mechanism and Consequences for PWR Safety Analysis", Proc. ANS/ENS Topical Meeting on Reactor Safety Aspects of Fuel Behavior, Sun Valley, Idaho, USA, August 2-6, 1981, Vol. 2, pp. 342-353

/10/ R.P. Elliot, Constitution of Binary Alloys, First Supplement (McGraw-Hill, New York), 1965.

/11/ V.F. Urbanic, T.R. Heidrick, "High-Temperature Oxidation of Zircaloy-2 and Zircaloy-4 in Steam", Journal of Nuclear Materials, 75, 1978, pp. 251-261.

/12/ A.E. Aly, Oxidation of Zircaloy-4 Tubing in Steam at 1350 to 1600°C, KfK 3358, May 1982.

/13/ R. R. Biederman, R.G. Ballinger, W.G. Dobson, A Study of Zircaloy-4 - Steam Oxidation Reaction Kinetics, EPRI NP-225, Electric Power Research Institute, September, 1976.

/14/ P. Hofmann, H.J. Neitzel; "External and Internal Reaction of Zircaloy Tubing with Oxygen and UO_2 and its Modeling", Fifth International Meeting on "Thermal Nuclear Reactor Safety",September 9-13, 1984, Karlsruhe, FRG.

/15/ P. Hofmann et al., "Mechanisches und chemisches Verhalten von Zircaloy-4-Hüllrohren und UO_2-Brennstoff bei hohen Temperaturen", PNS-Jahresbericht 1983, KfK 3450 (1984) pp. 4200/126-145.

Table 1: Zircaloy-4 Chemical Composition (wt.%)

Sn	1.57
Fe	0.22
Cr	0.10
Ni	0.0035
H	0.0006
C	0.014
N	0.0028
O	0.13
Zr	balance

Table 2: Measured mass increase, thickness of ZrO_2 layer and thickness of (ZrO_2+α-Zr(O)) double layer as functions of temperature and time (25 Vol.% O_2 + 75 Vol.% Ar)

Specimen Nr.	Temperature (°C)	Time (min)	Equivalent Isothermal Oxidation Time (sec)	Mass Increase (mg/cm²)	ZrO_2 (µm)	ZrO_2/α-Zr
46	900	2	143	1.29	6.9	12.9
47		5	322	1.89	9.5	17.8
48		10	622	2.34	12.5	22.8
49		15	922	2.81	14.9	27.6
50		20	1222	3.05	15.9	30.0
51		30	1822	3.45	17.1	36.0
52		45	2722	4.05	20.6	42.0
53		60	3622	4.30	21.8	46.0
1	996	2	151	3.21	17.3	27.4
2		5	331	4.38	24.1	38.3
42		10	631	5.94	32.5	52.1
4		15	931	7.19	38.0	60.5
43		20	1231	8.03	45.1	72.0
45		30	1831	8.97	53.3	84.5
6		45	2731	11.59	64.6	104.6
8		60	3631	14.09	68.7	111.5
9	1100	2	138	5.71	30.1	53.0
10		5	318	8.75	49.5	83.1
11		10	618	11.89	65.3	109.8
12		15	918	14.25	77.8	129.8
13		20	1218	16.12	88.4	146.5
14		30	1818	19.48	106.0	177.1
15		45	2718	23.43	128.8	216.1
16		60	3618	27.66	150.8	254.3

Table 2: continued

Table 2: continued - 1

Specimen Nr.	Temperature (^{o}C)	Time (min)	Equivalent Isothermal Oxidation Time (sec)	Mass Increase (mg/cm^2)	ZrO_2 (μm)	ZrO_2+α (μm)
17	1200	2	144	9.49	48.9	95.3
18		5	315	12.83	65.1	129.6
19		10	615	17.67	91.6	180.1
20		15	915	20.80	107.7	216.2
21		20	1215	23.94	123.5	244.0
22		30	1815	28.92	150.0	315.0
23		45	2715	35.85	190.5	-
24		60	3615	41.11	220.5	-
25	1300	2	132	13.20	62.1	144.3
26		5	308	18.46	88.9	206.5
27		10	608	25.00	121.6	-
28		15	908	30.02	150.7	-
29		20	1208	34.71	173.9	-
30		30	1808	42.19	221.0	-
31		45	2708	51.32	296.0	-
32		60	3608	58.12	348.4	-
41	1400	2	137	18.86	88.8	213.5
34		5	317	26.53	127.3	-
35		10	617	36.07	182.9	-
36		15	917	43.33	235.2	-
37		20	1217	49.04	283.9	-
38		30	1817	57.79	359.8	-
39		45	2717	69.57	457.5	-
40		60	3617	74.74	513.1	-
79	1500	2	130	31.53	175.8	-
80		5	313	41.11	229.8	-
81		10	605	51.54	333.8	-
82		15	909	59.04	397.5	-
83		20	1210	65.46	453.8	-
84		30	1810	74.45	510.0	-

Table 3: Parabolic rate law constants for oxidation reaction of Zircaloy-4 in a 25 Vol.% O_2/75 Vol.% Ar gas mixture(determined graphically)

Temperature (^oC)	Mass Increase (K_w) (g^2/cm^4s)	Thickness of ZrO_2 ($K\delta$) (cm^2/s)	Thickness of (ZrO_2+α-Zr(O)) (K_ξ) (cm^2/s)	Time Range (min)
900	$9.30\ (\pm 1.73)\times 10^{-9}$	$2.44\ (\pm 0.37)\times 10^{-9}$	$8.60\ (\pm 1.24)\times 10^{-9}$	5 ∿ 20
996	$5.10\ (\pm 0.71)\times 10^{-8}$	$1.64\ (\pm 0.11)\times 10^{-8}$	$4.17\ (\pm 0.27)\times 10^{-8}$	5 ∿ 45
1100	$2.22\ (\pm 0.20)\times 10^{-7}$	$6.91\ (\pm 0.81)\times 10^{-8}$	$1.95\ (\pm 0.23)\times 10^{-7}$	2 ∿ 60
1200	$4.92\ (\pm 0.31)\times 10^{-7}$	$1.30\ (\pm 0.06)\times 10^{-7}$	$5.19\ (\pm 0.29)\times 10^{-7}$	5 ∿ 60
1300	$1.05\ (\pm 0.07)\times 10^{-6}$	$2.57\ (\pm 0.14)\times 10^{-7}$	1.38×10^{-6}	5 ∿ 30
1400	$2.29\ (\pm 0.31)\times 10^{-6}$	$5.87\ (\pm 0.76)\times 10^{-7}$	3.33×10^{-6}	2 ∿ 20
1500	$4.47\ (\pm 0.93)\times 10^{-6}$	$1.77\ (\pm 0.08)\times 10^{-6}$		5 ∿ 20

The indicated rate law constants are average values determined graphically. The upper and lower values of the scatter band are boundary lines passing through the origin covering all data points.

Table 4: Parabolic rate law constants determined by the method of least squares

Temperature (^{o}C)	Mass Increase (K_w) ($g^2/cm^4 s$)	Thickness of ZrO_2 (K_δ) (cm^2/s)	Thickness of ZrO_2+α-Zr(O) (K_ξ) (cm^2/s)	Time Range (min)
900	8.46×10^{-9}	2.33×10^{-9}	8.07×10^{-9}	5 ∿ 20
996	5.01×10^{-8}	1.58×10^{-8}	4.05×10^{-8}	5 ∿ 45
1100	2.12×10^{-7}	6.34×10^{-8}	1.78×10^{-7}	2 ∿ 60
1200	4.72×10^{-7}	1.31×10^{-7}	5.22×10^{-7}	5 ∿ 60
1300	1.00×10^{-6}	2.57×10^{-7}	1.38×10^{-6}	5 ∿ 30
1400	2.07×10^{-6}	6.02×10^{-7}	3.33×10^{-6}	2 ∿ 20
1500	3.97×10^{-6}	1.74×10^{-6}		5 ∿ 20

Table 5: Temperature dependence of the parabolic rate constants determined graphically and by the least squares method

K_p	Graphic Method	Least Squares	Temp. Range
Mass Increase	$K_W = 24.12 \exp(-211,112/RT)$	$K_W = 31.37 \exp(-214,435/RT)$	900 ~ 1100°C
K_W [$g^2/cm^4 \cdot s$]	$K_W = 0.135 \exp(-152,805/RT)$	$K_W = 0.092 \exp(-148,783/RT)$	1100 ~ 1500°C
Thickness of ZrO_2 K_δ [cm^2/s]	$K_\delta = 21.52 \exp(-222,682/RT)$	$K_\delta = 15.88 \exp(-220,077/RT)$	900 ~ 1100°C
	$K_\delta = 8.27 \times 10^{-4} \exp(-107,230/RT)$	$K_\delta = 3.05 \times 10^{-3} \exp(-123,138/RT)$	1100 ~ 1200°C
	$K_\delta = 6.14 \times 10^{-3} \exp(-131,775/RT)$	$K_\delta = 5.48 \times 10^{-3} \exp(-130,294/RT)$	1200 ~ 1300°C
	$K_\delta = 0.259 \exp(-180,709/RT)$	$K_\delta = 0.395 \exp(-186,230/RT)$	1300 ~ 1400°C
	$K_\delta = 158.2 \exp(-269,890/RT)$	$K_\delta = 77.08 \exp(-259,539/RT)$	1400 ~ 1500°C
	$K_\delta = 8.98 \times 10^{-3} \exp(-135,419/RT)$	$K_\delta = 1.48 \times 10^{-2} \exp(-141,837/RT)$	1100 ~ 1400°C
Thickness of (ZrO_2+α-Zr(O)) K_ξ [cm^2/s]	$K_\xi = 14.96 \exp(-207,521/RT)$	$K_\xi = 11.92 \exp(-205,771/RT)$	900 ~ 1100°C
	$K_\xi = 1.549 \exp(-181,885/RT)$	$K_\xi = 2.322 \exp(-187,253/RT)$	1100 ~ 1400°C

R = 8.314 J/mol·K, T = absolute Temperature in K

Table 6: Mass increase of Zircaloy-4 oxidized at 1200°C in different oxidizing atmospheres as a function of time

Time (min)	Mass Increase (mg/cm^2)		
	10% O_2 + 90% Ar (Vol.%)	25% O_2 + 75% Ar (Vol.%)	100% O_2
2	8.70	9.49	8.88
5	12.73	12.83	13.38
10	17.20	17.67	17.58
15	20.63	20.80	20.94
20	23.79	23.94	23.66
30	29.13	28.92	31.41
45	35.53	35.85	34.42
60	39.43	41.11	40.34

Table 7: Data of the MONA experiments and the evaluated temperatures (MONA experiments: UO_2/Zry interaction experiments under oxidizing conditions /14,15/).

Nominal Test Temperature of MONA (°C)	Oxidation Time (min)	Average Oxide Layer Thickness (µm)	Evaluated Temperature graphical (°C)	Evaluated Temperature least squares (°C)
900	11	13.4	902	904
	31	21.4	897	899
1020	4	27.6	1044	1049
	11	47.5	1049	1053
	31	81.7	1052	1057
1100	4	48.0	1150	1156
	11	78.5	1146	1152
	31	130.3	1143	1149
1200	4	68.6	1258	1258
	11	110.7	1250	1250
	31	198.6	1270	1270
1300	4	89.8	1330	1330
	11	145.2	1325	1324
	31	267.6	1347	1345
1400	4	136.6	1424	1422
	11	227.5	1425	1423
	31*	462.4	1459*	1460*

* : reference data: Evaluation is available for oxidation times ranging from 2 to 20 min at 1400°C (see Table 3).

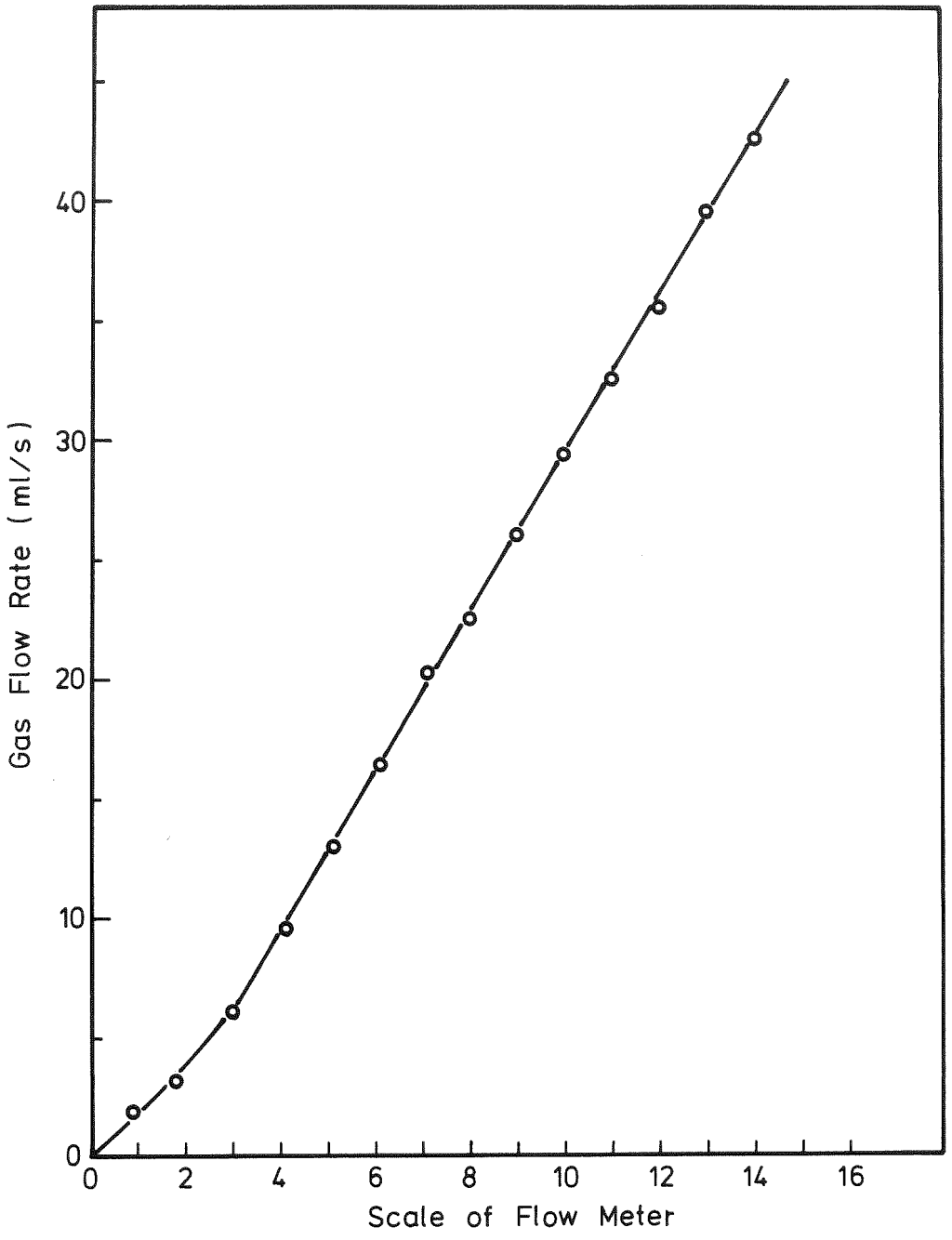

Fig. 1: Gas flow rate as a function of the scale of flow meter. (25 Vol.% Oxygen + 75 Vol.% Argon, Rotameter Nr. L 6.3/ 250-4221).

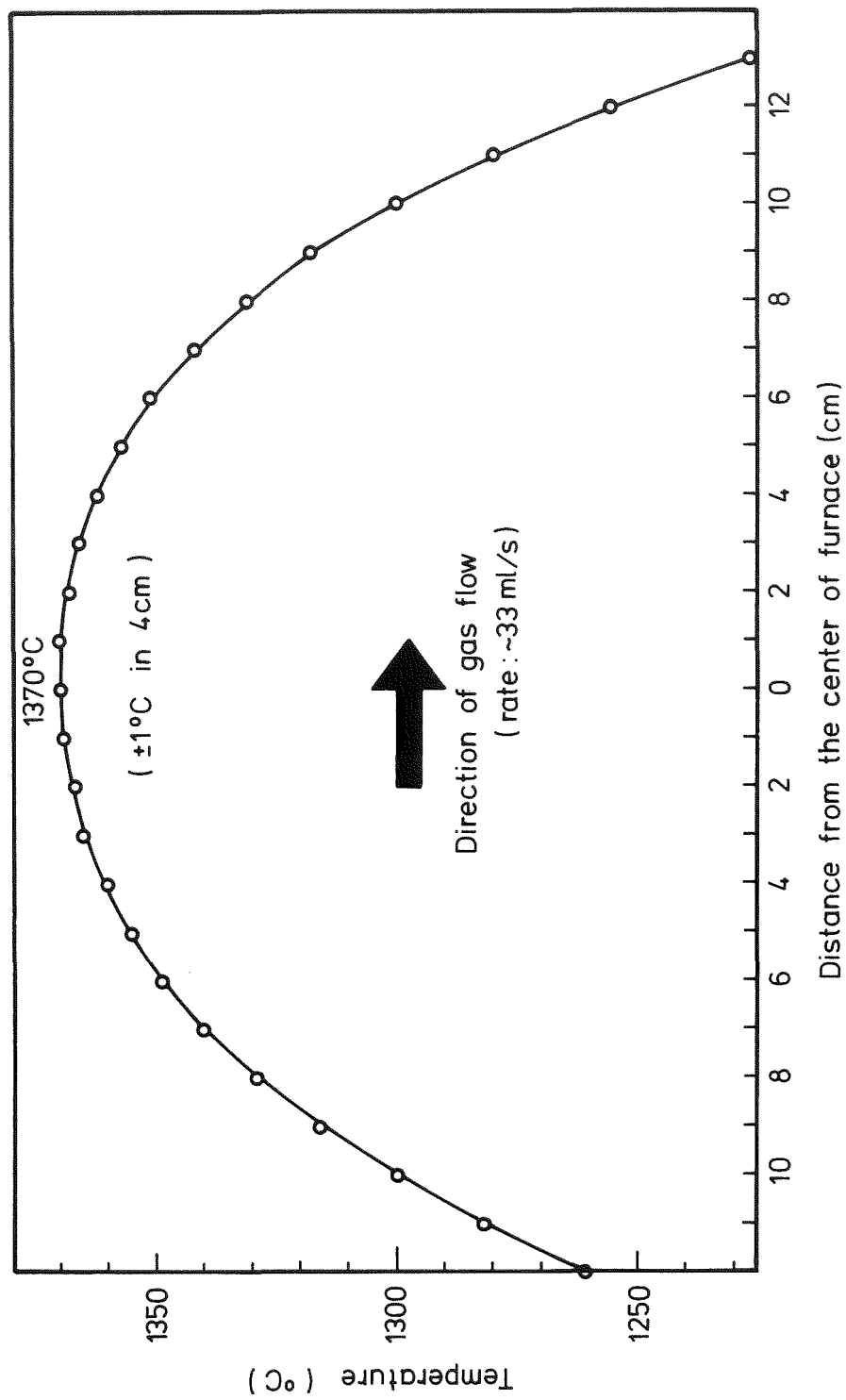

Fig. 2: Axial temperature profile in the test furnace.

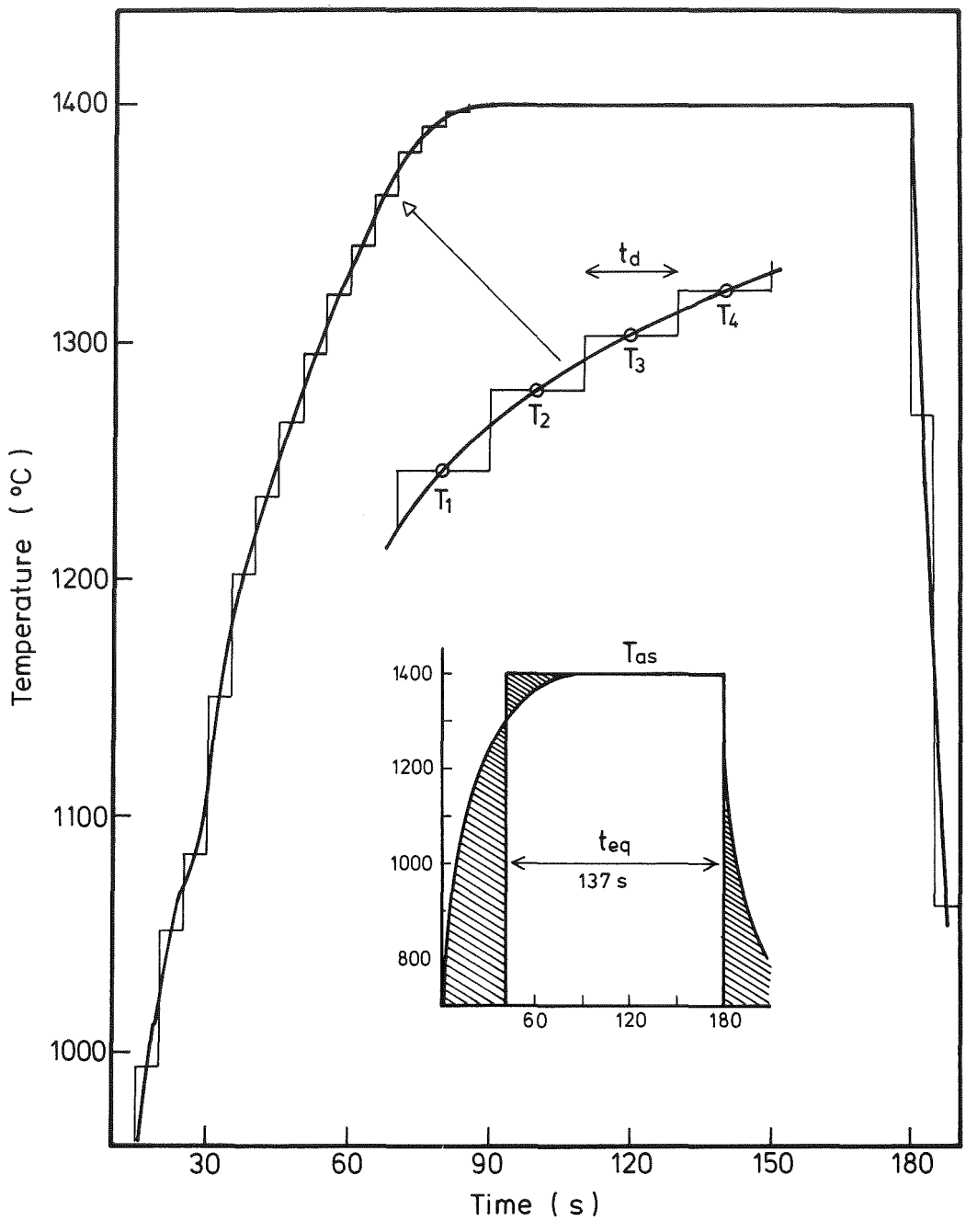

Fig. 3: Temperature transient for isothermal oxidation test at 1400°C for 2 min and normalization to equivalent isothermal oxidation time.

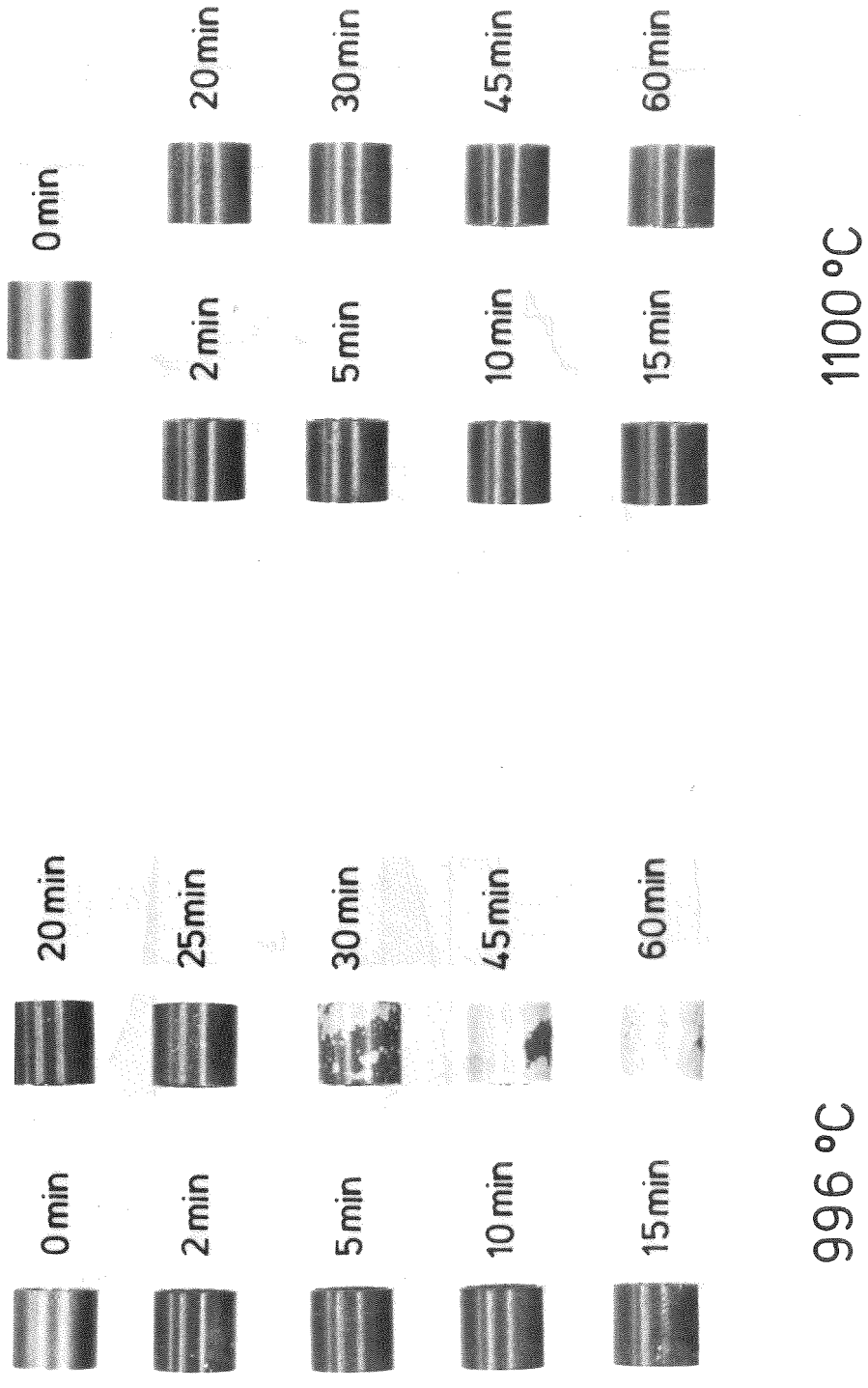

Fig. 4: Visual appearance of Zircaloy-4 specimens oxidized at 996 and 1100°C for 2 to 60 min.

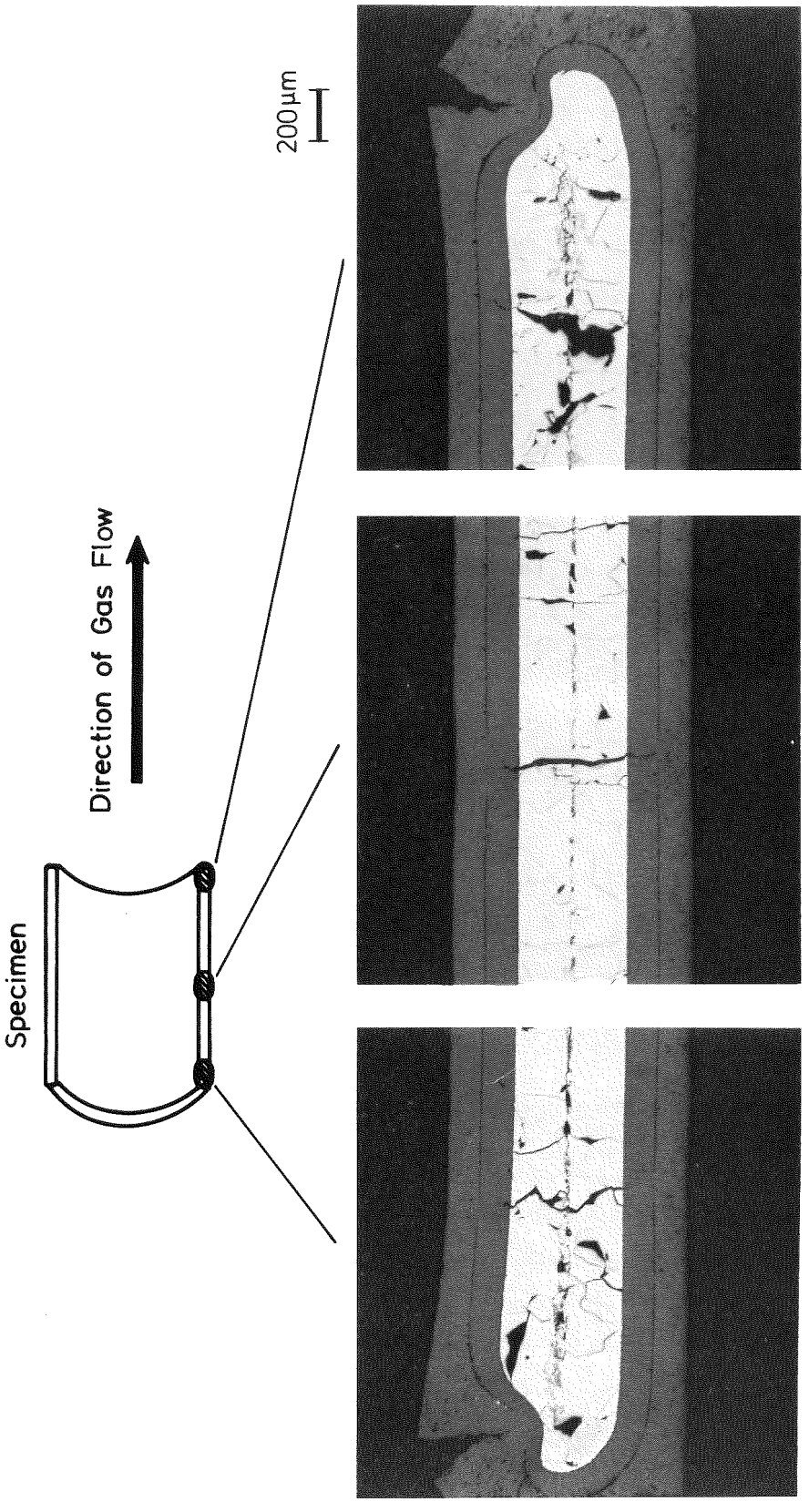

Fig. 5: Oxide (ZrO_2) film formed uniformly along the specimen length. Oxidation at 1400°C for 15 min.

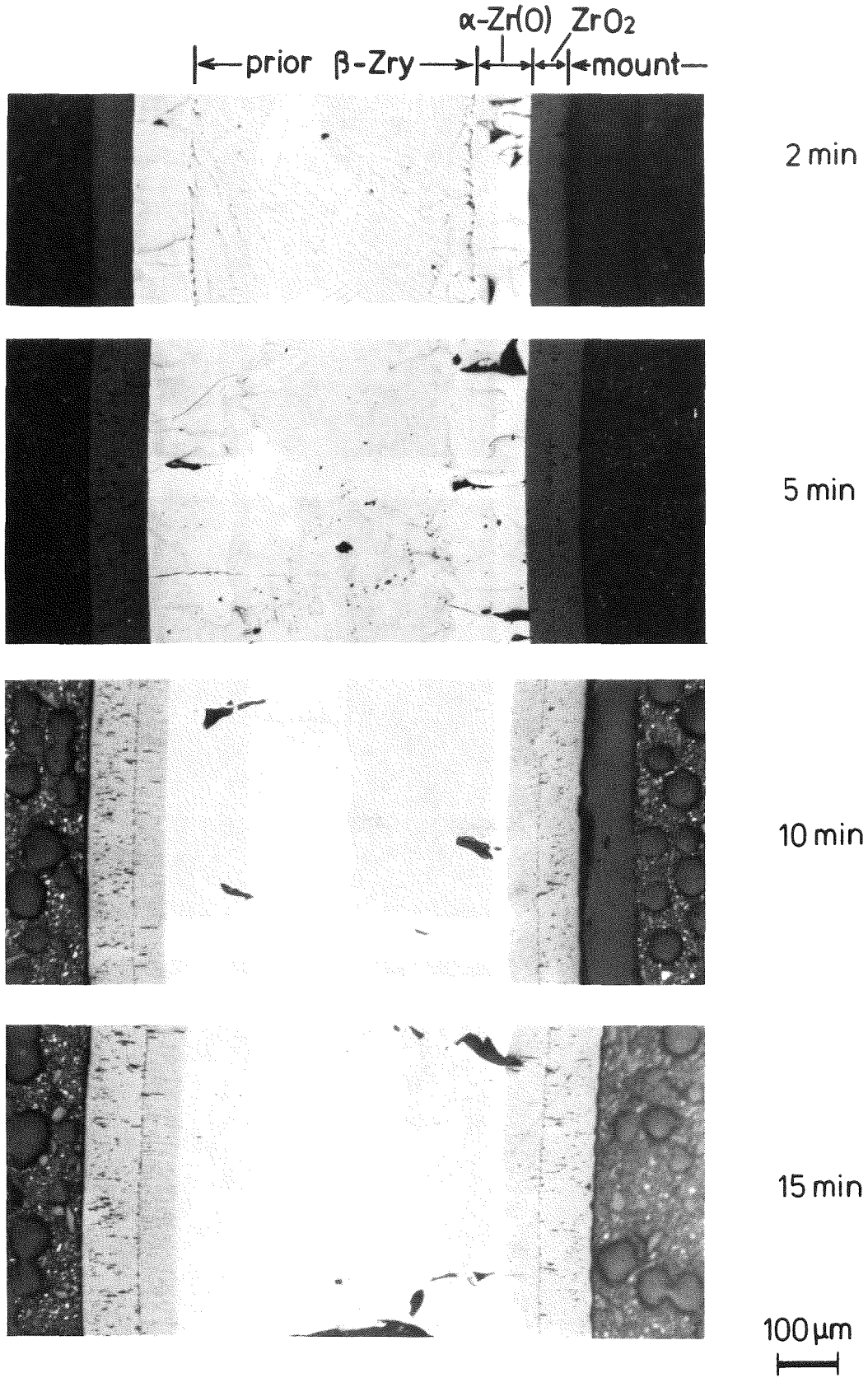

Fig. 6: Photomicrographs of Zircaloy-4 oxidized at 1300°C for 2 to 15 min in a (25 Vol.% O_2/75 Vol.% Ar) gas mixture.

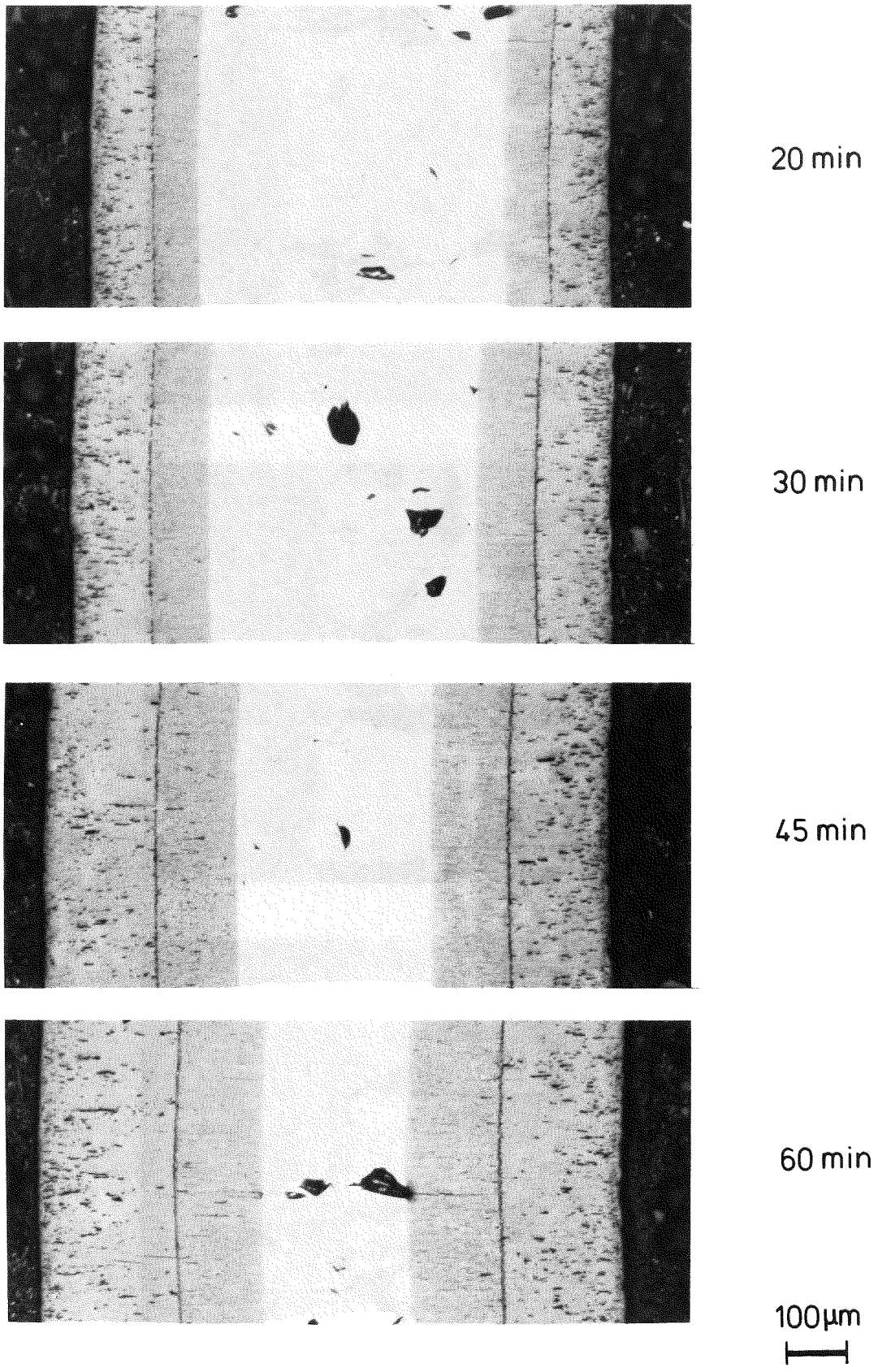

Fig. 7: Photomicrographs of Zircaloy-4 oxidized at 1300°C for 20 to 60 min in a (25 Vol.% O_2/75 Vol.% Ar) gas mixture.

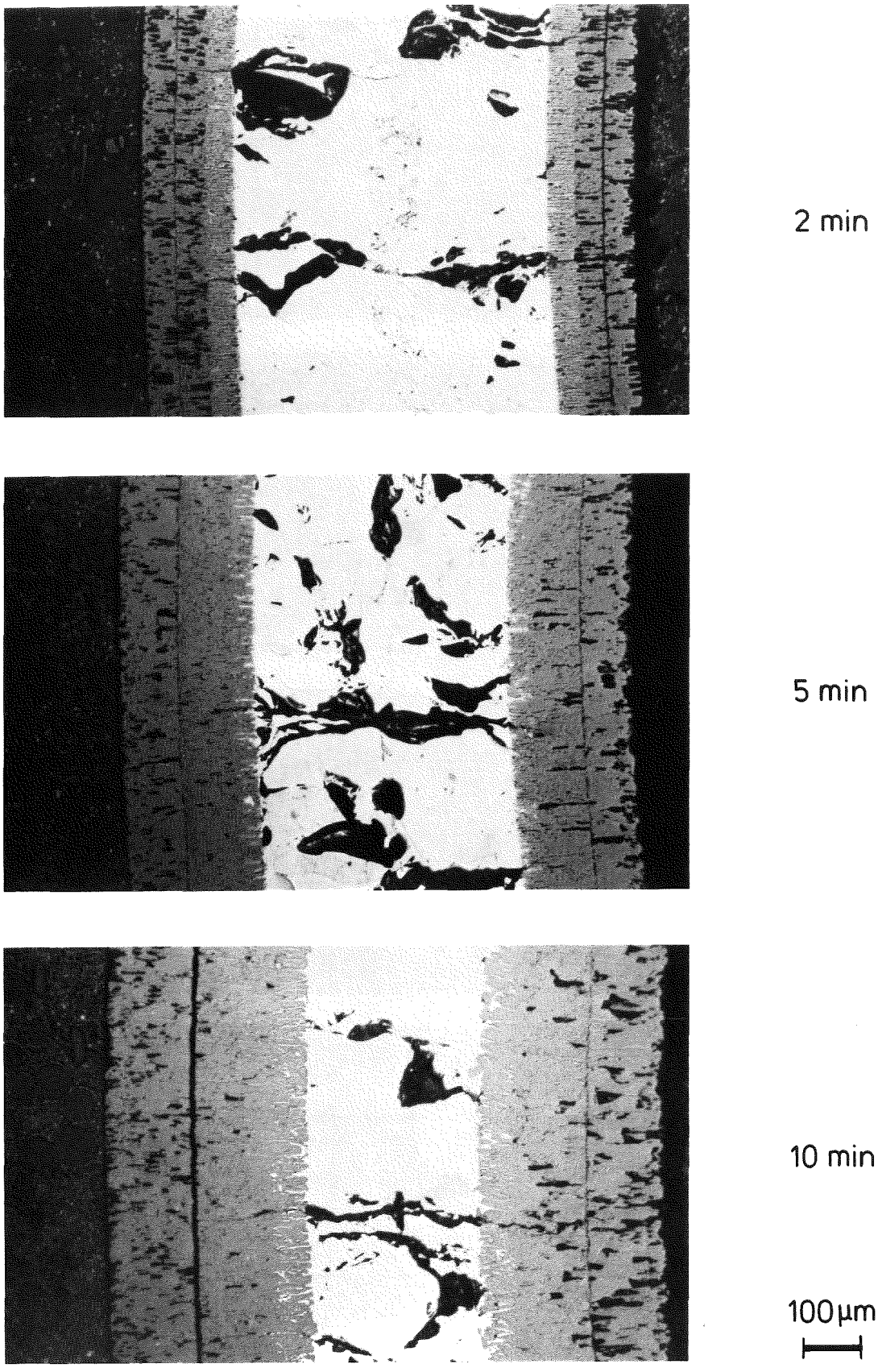

Fig. 8: Photomicrographs of Zircaloy-4 oxidized at 1500°C for 2 to 10 min in a (25 Vol.% O_2/75 Vol.% Ar) gas mixture.

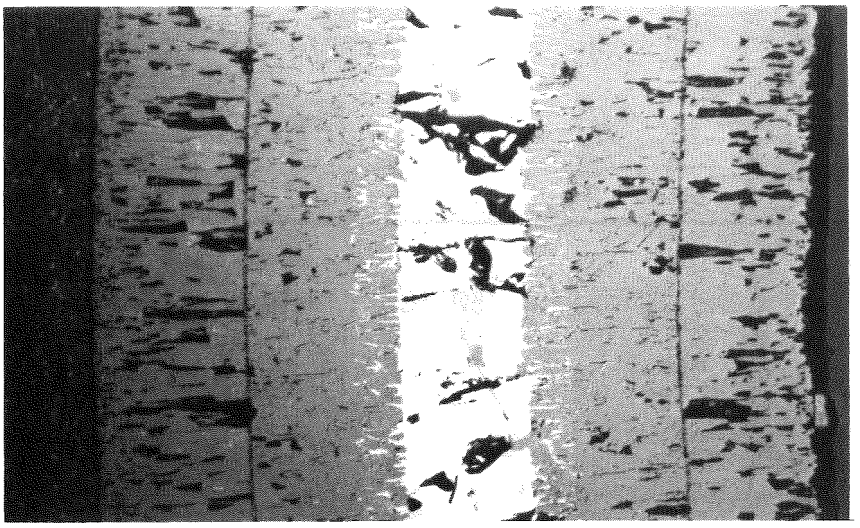

15 min

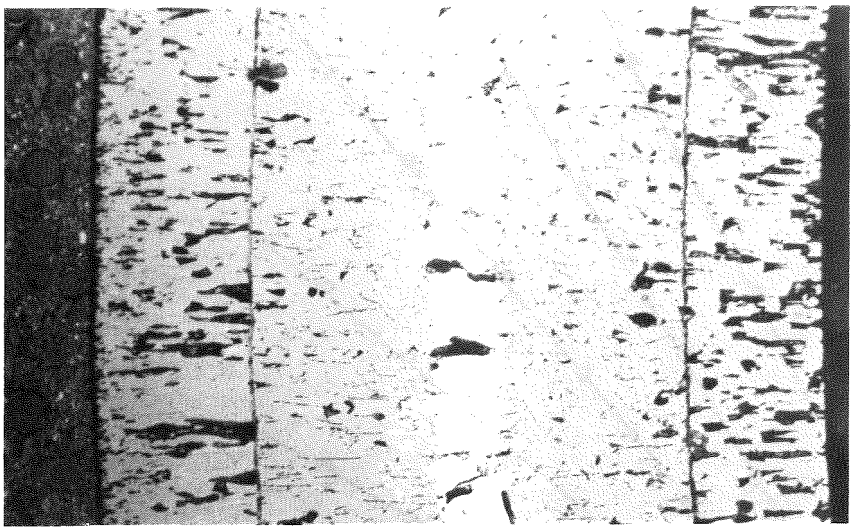

20 min

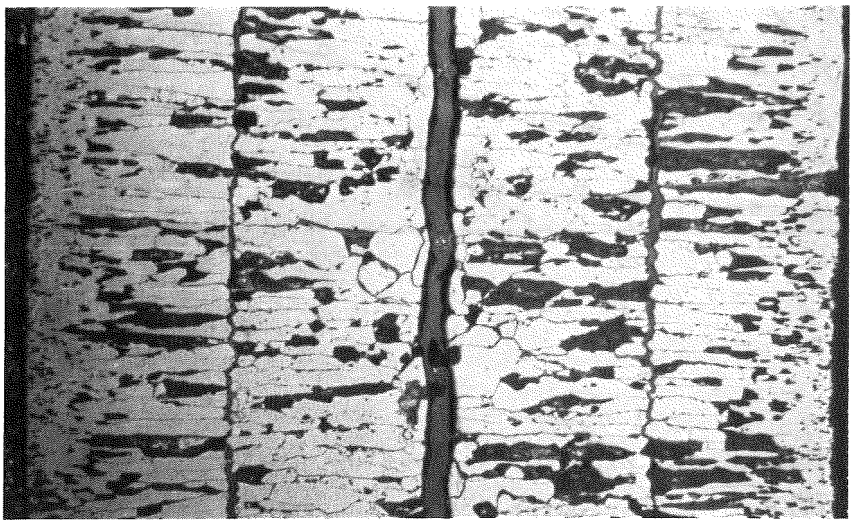

30 min

100 µm

Fig. 9: Photomicrographs of Zircaloy-4 oxidized at 1500°C for 15 to 30 min in a (25 Vol.% O_2/75 Vol.% Ar) gas mixture.

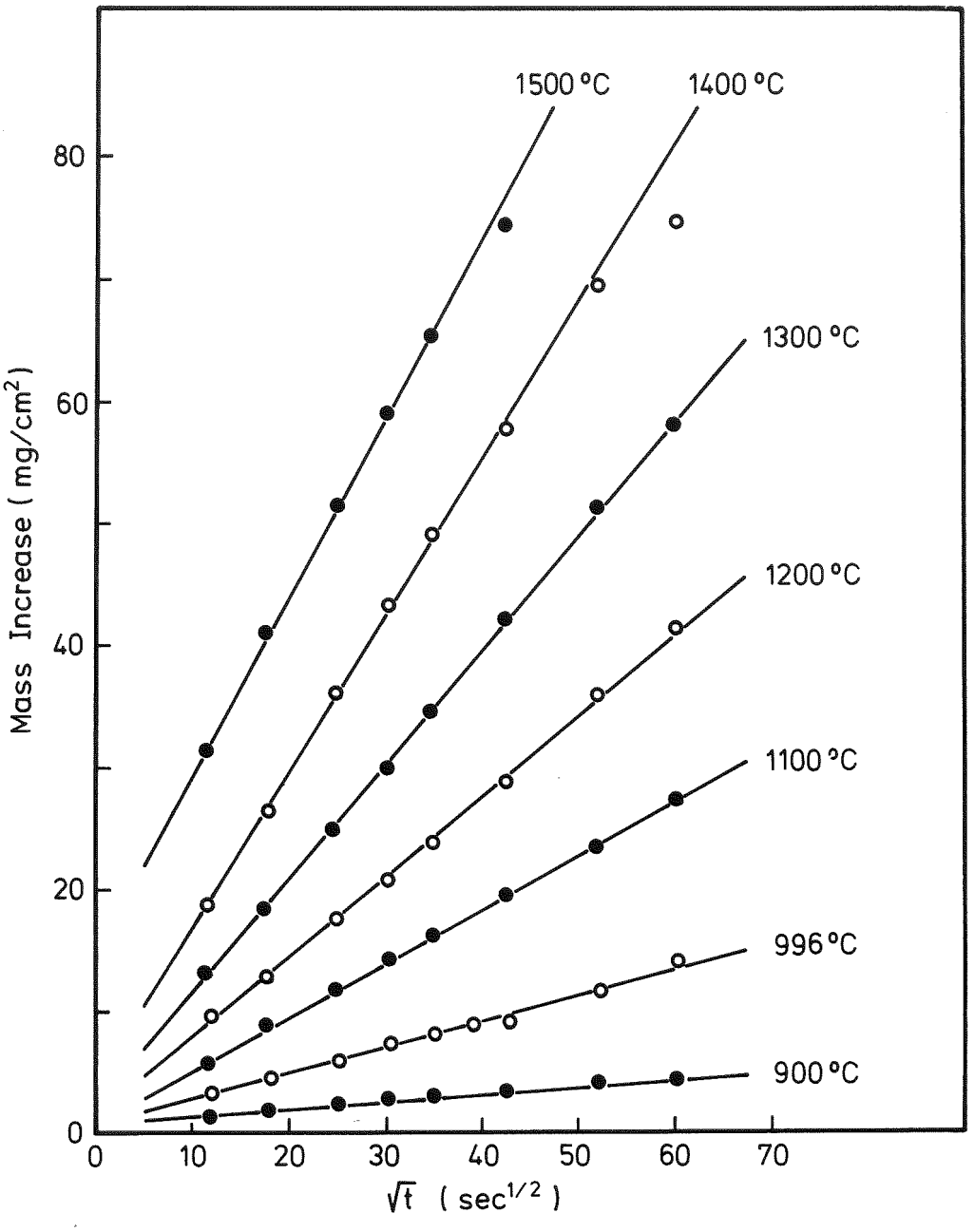

Fig. 10: Mass increase of Zircaloy-4 cladding specimens oxidized at different temperatures versus the square root of oxidation time ($\sqrt{t}$).

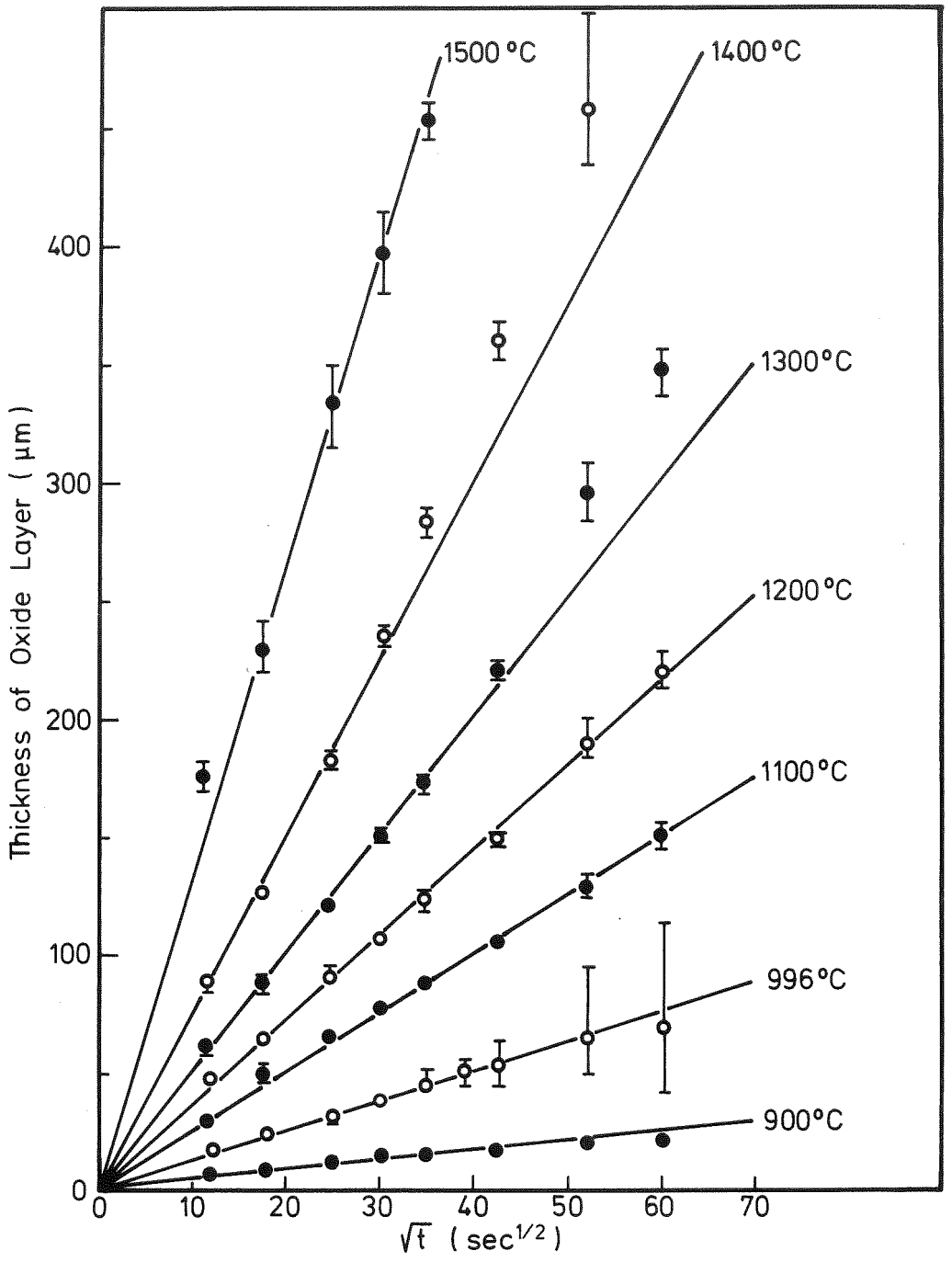

Fig. 11: Increase of oxide (ZrO_2) layer thickness as a function of the square root of oxidation time ($\sqrt{t}$).

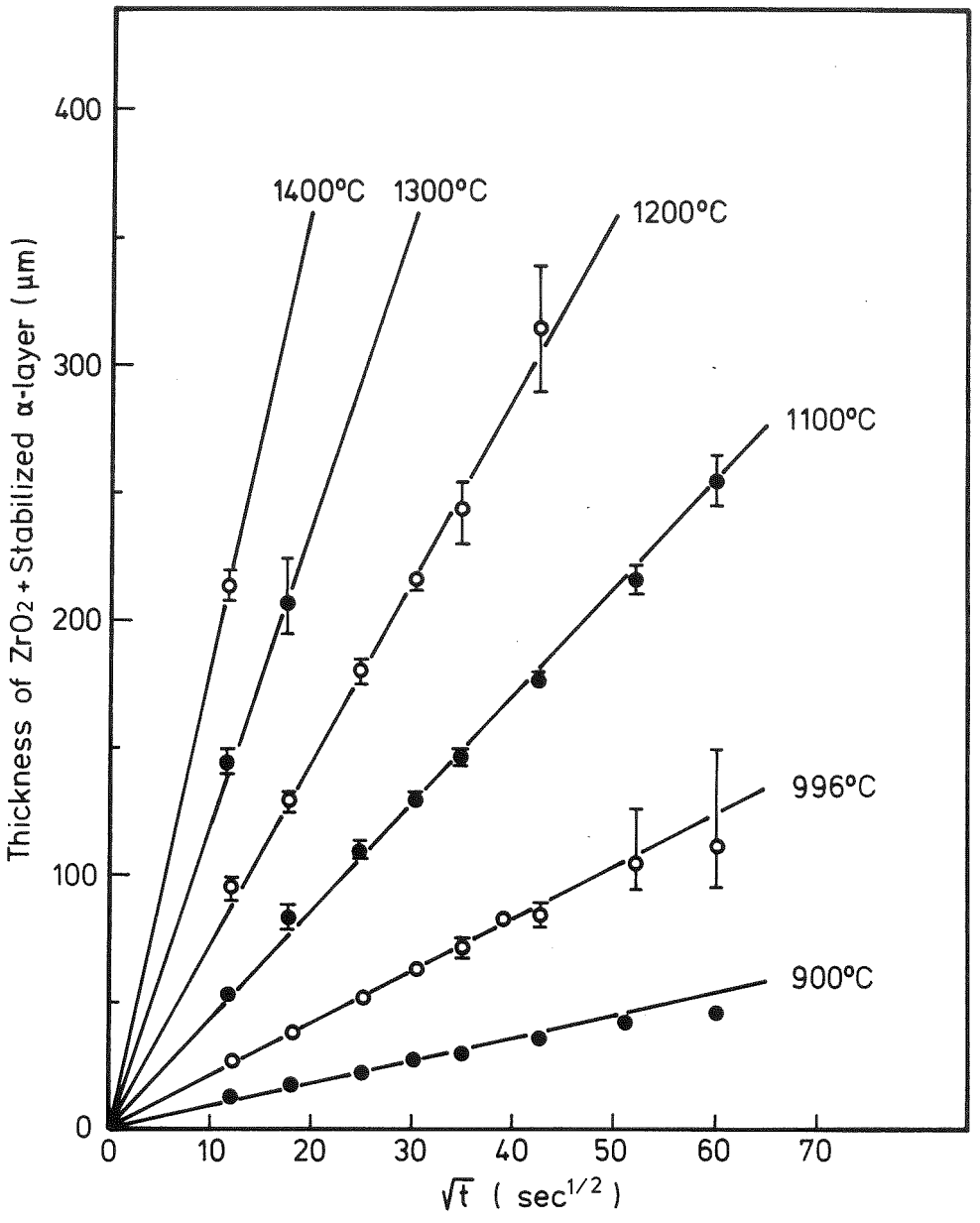

Fig. 12: Increase of (ZrO_2+α-Zr(O)) double layer thickness as a function of the square root of oxidation time ($\sqrt{t}$).

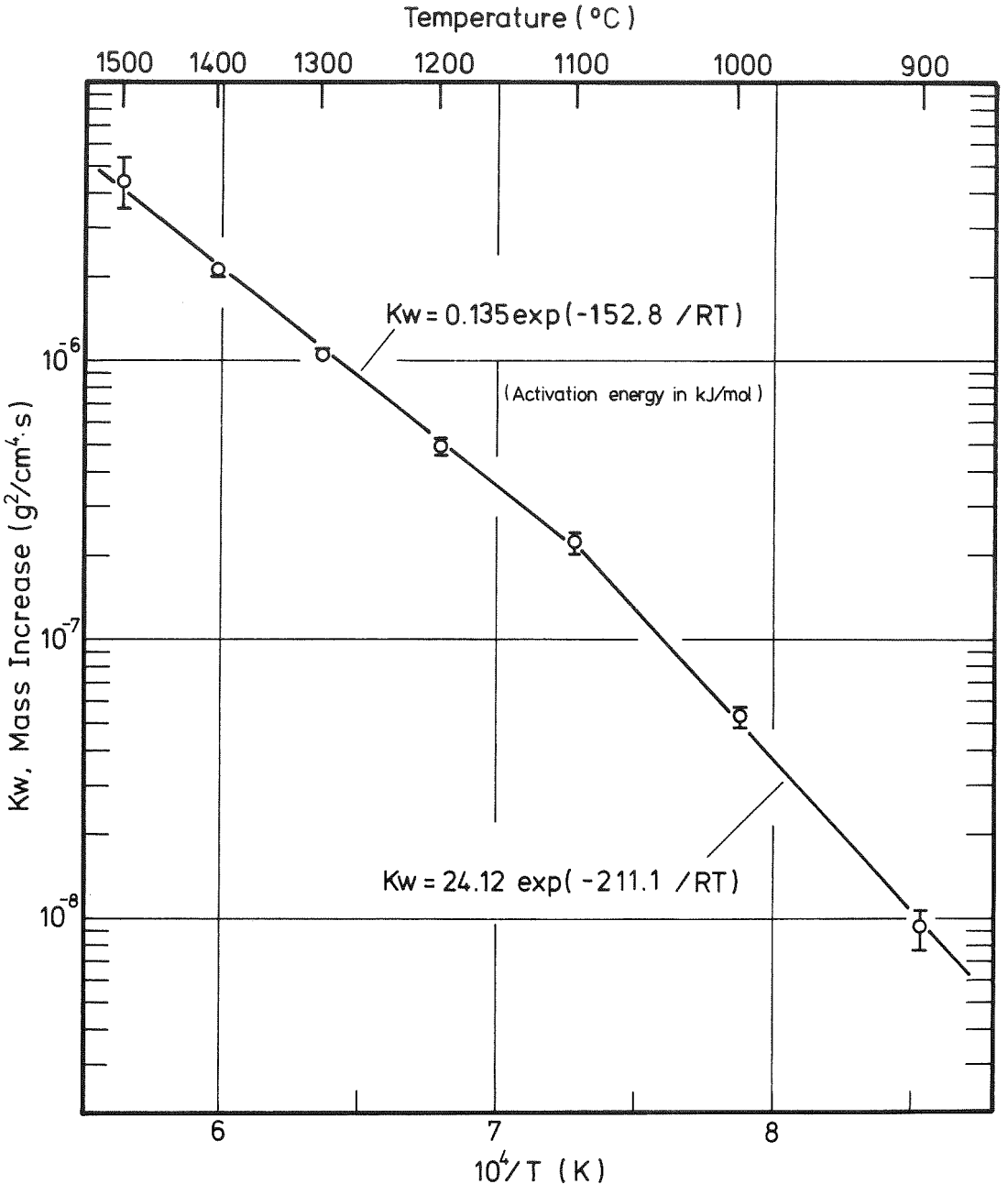

Fig. 13: Arrhenius plot of the parabolic rate constants for mass increase from 900 to 1500°C.

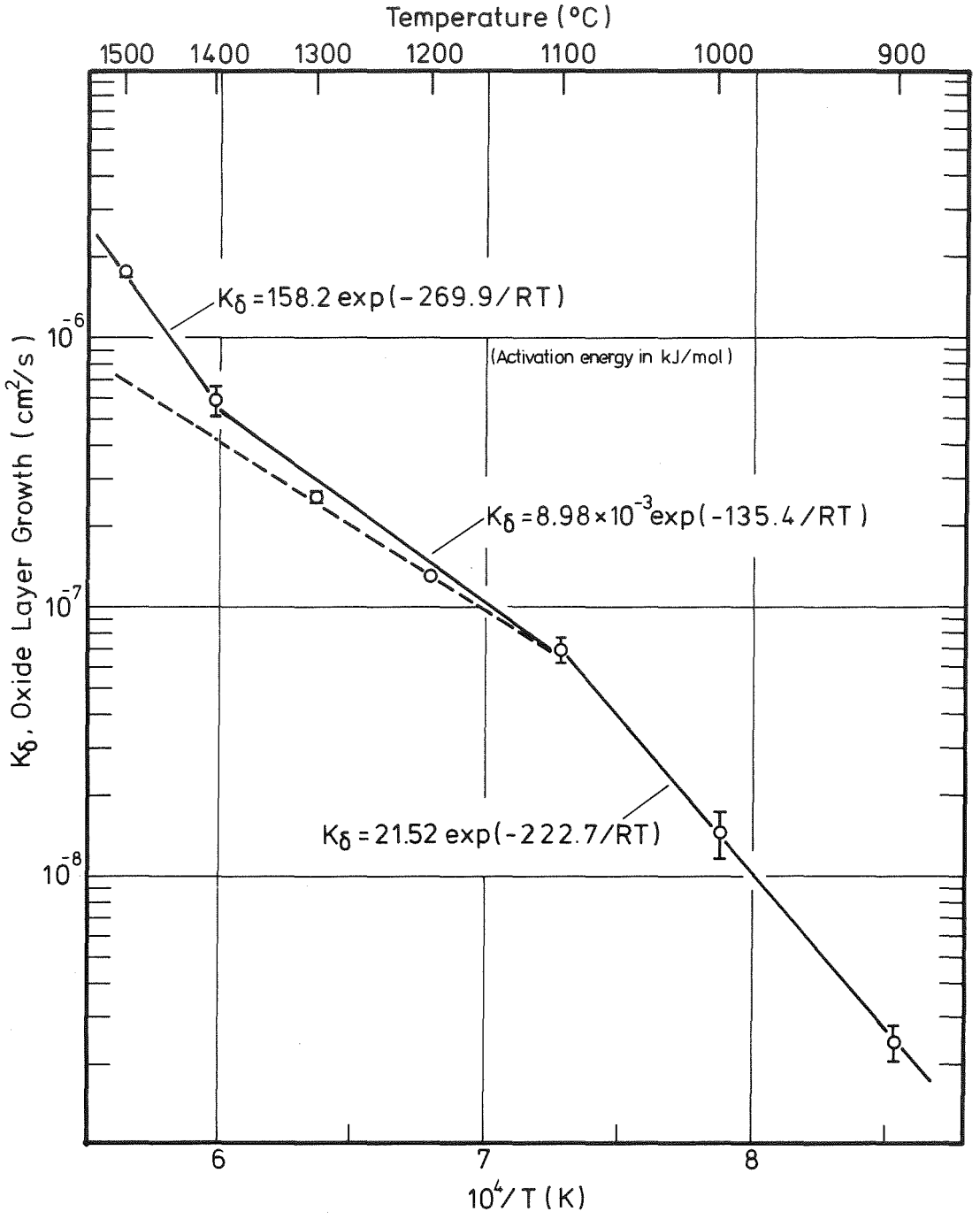

Fig. 14: Arrhenius plot of the parabolic rate constants for oxide layer growth from 900 to 1500°C.

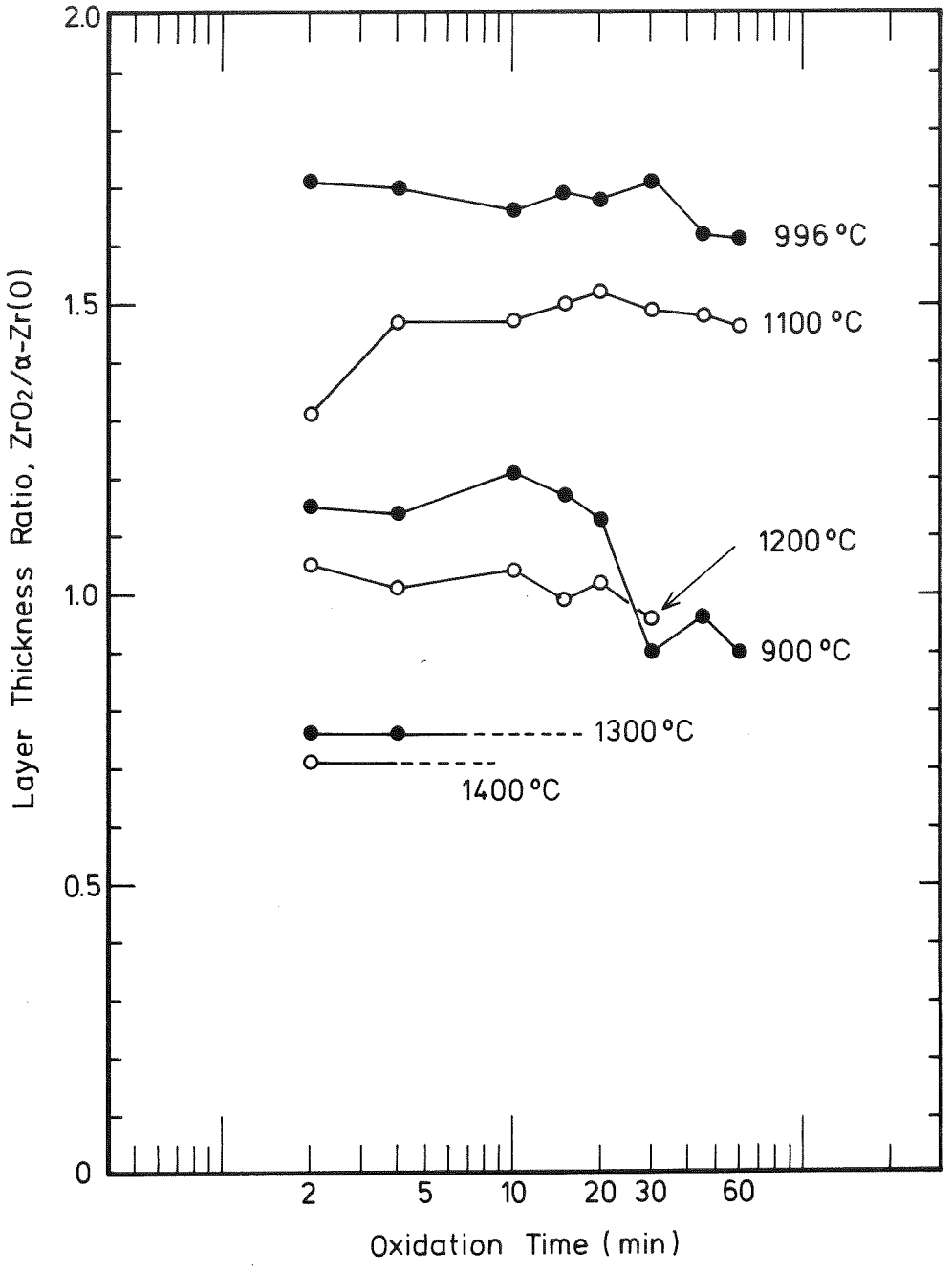

Fig. 15: Variation of layer thickness ratio of ZrO_2/oxygen-stabilized α-Zr(O) as a function of oxidation time.

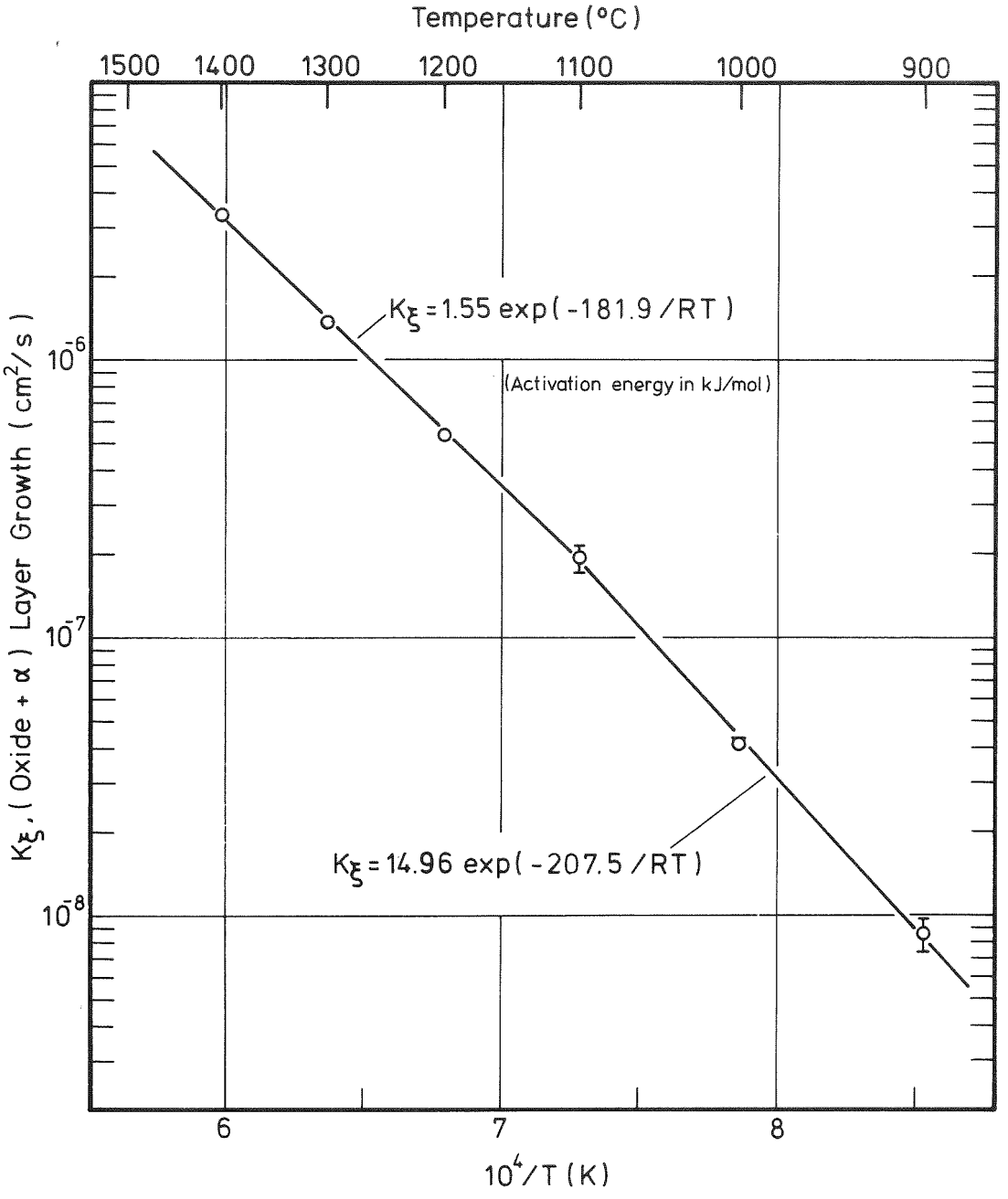

Fig. 16: Arrhenius plot of the parabolic rate constants for (ZrO_2+ α-Zr(O)) layer growth from 900 to 1400°C.

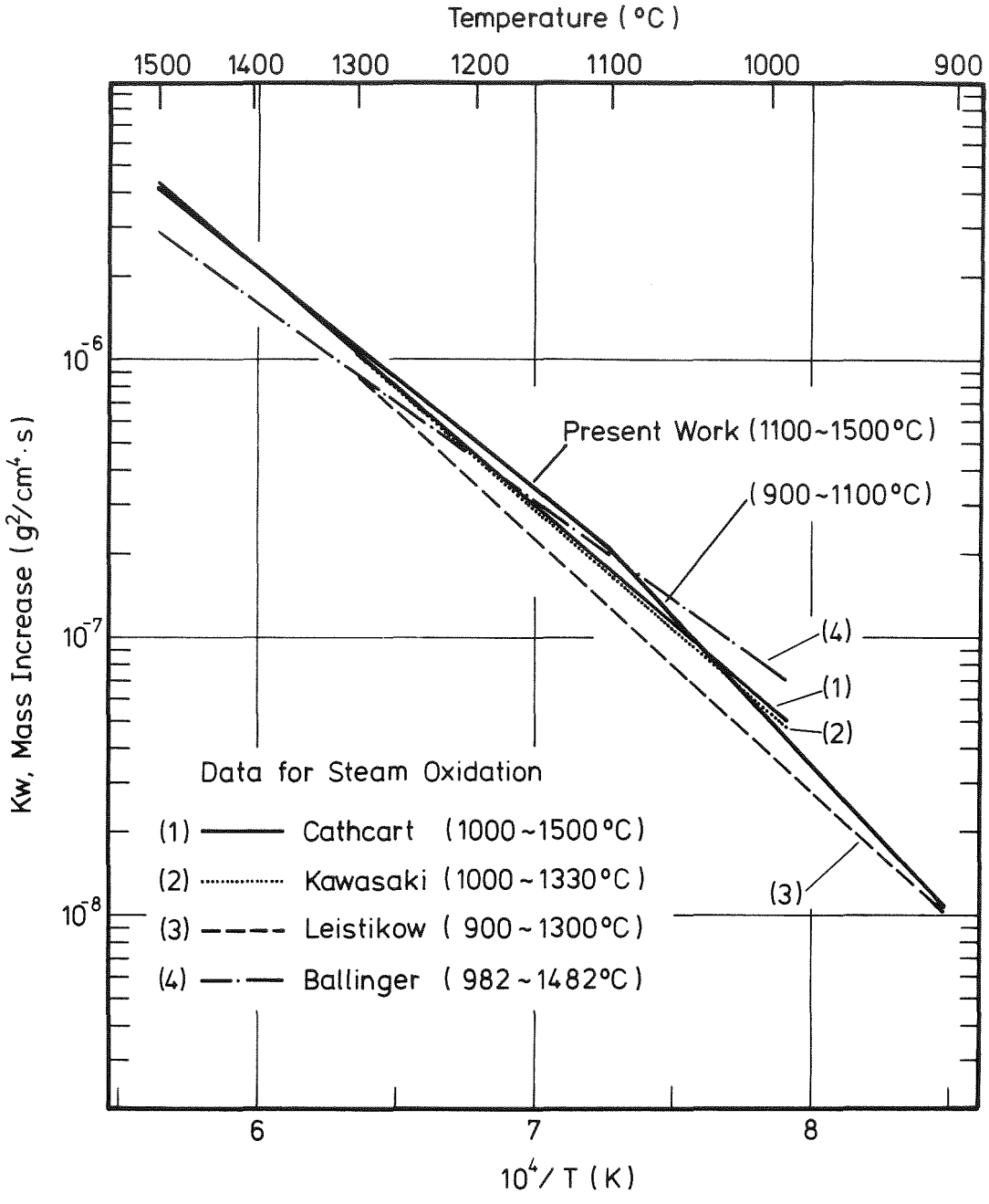

Fig. 17: Comparison of oxidation rate of Zircaloy-4 measured in steam and in a (25 Vol.% O_2/75 Vol.% Ar) gas mixture (present work).

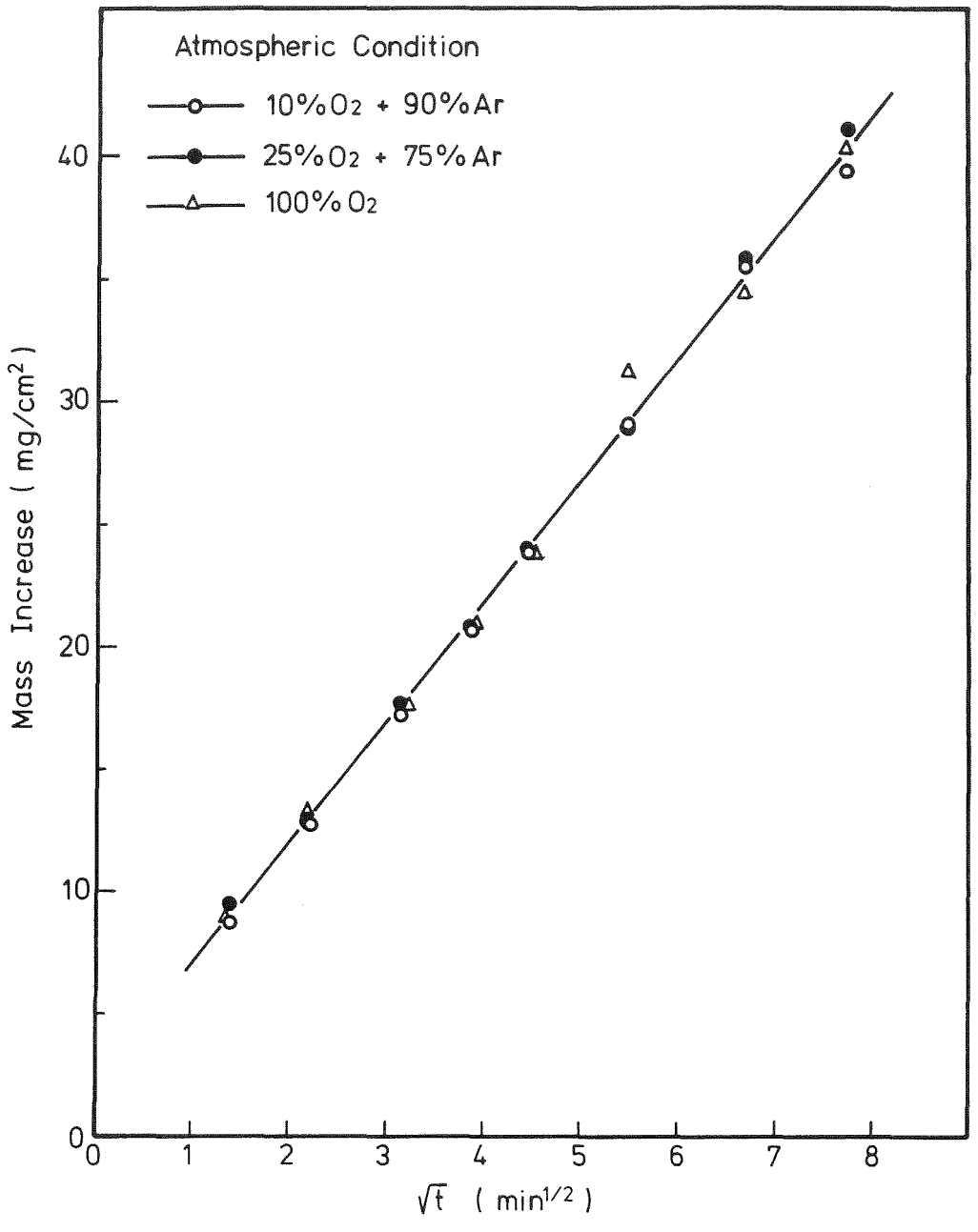

Fig. 18: Mass increase of Zircaloy-4 cladding specimens oxidized at 1200°C as a function of the square root of oxidation time ($\sqrt{t}$) at three different oxygen to argon ratios.

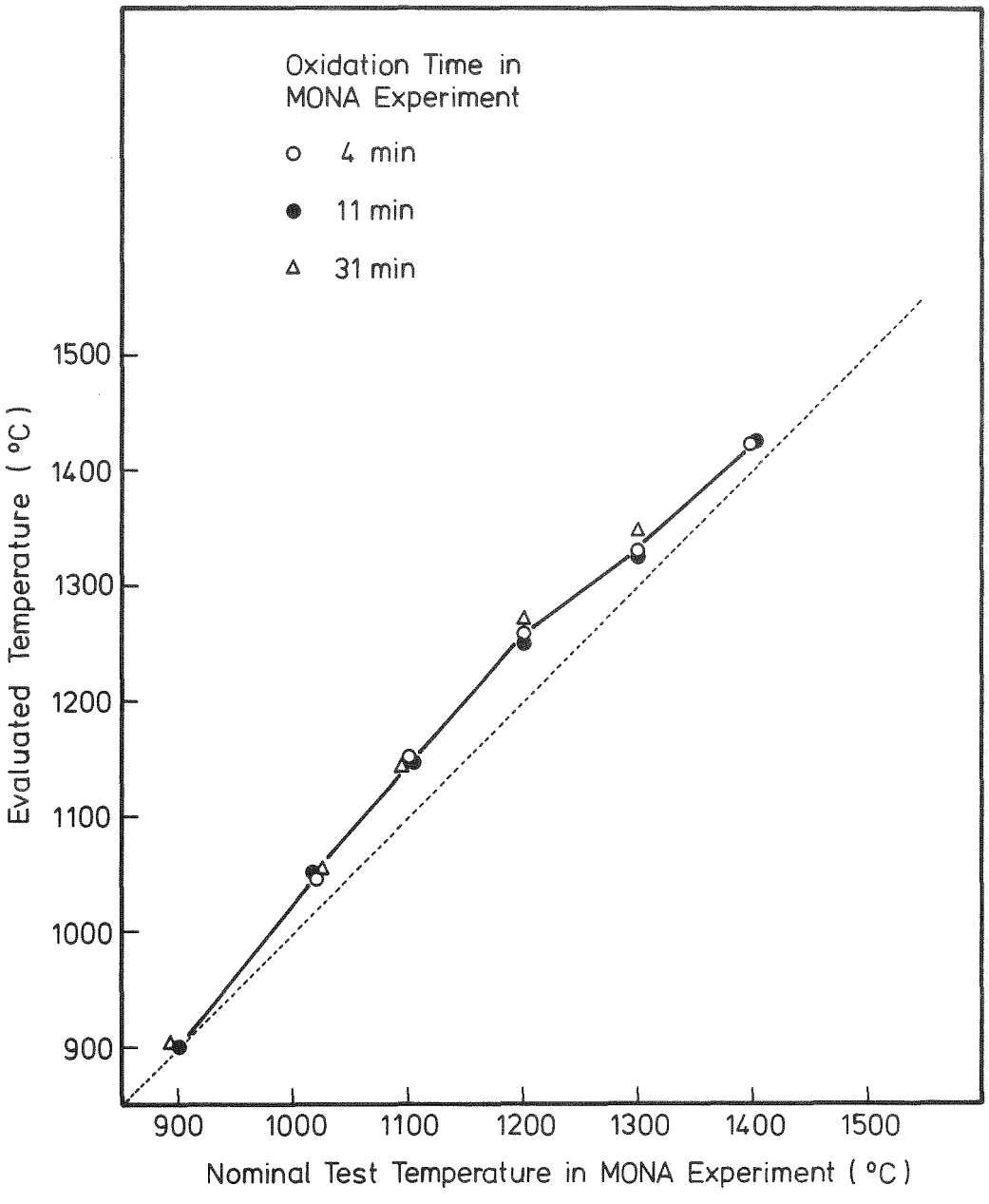

Fig. 19: Correlation between nominal test temperatures in the MONA experiments and the temperatures evaluated from the oxide layer thickness.